UNIVERSITY OF SOUTHAMPTON

FACULTY OF SCIENCE

PHYSICS

STUDIES OF HIGH T_c SUPERCONDUCTORS AND RELATED COMPOUNDS

R Madaiah

A thesis submitted for the degree of

Master of Philosophy

1988

CONTENTS

UNIVERSITY OF SOUTHAMPTON

FACULTY OF SCIENCE

PHYSICS

Master of Philosophy

Studies of high T_c superconductors and related compounds

by R Madaiah

ABSTRACT

The d.c. resistivities of unannealed and annealed $La_{2+x}Ba_{4-x}Cu_6O_{14\pm y}$ compounds have been measured in the temperature range 6K to 300K by the four probe technique. The unannealed compounds show a complex resistivity behaviour and are semiconducting at low temperatures. The annealed compounds exhibit a superconducting behaviour. The compound with x=0 has the highest transition temperature T_c (65K). The increase in La concentration results in a decrease of the transition temperature. The compound with x=0.8 does not show a superconducting behaviour down to 6K.

Measurements of resistivity on $Y_2La_xBa_{4-x}Cu_6O_{14\pm y}$ with x=0.2 and 0.6 have been compared with other compounds in the series. The compound with x=0.2 is found to have the highest critical temperature (93K).

These results in combination with the structural details provided by powder neutron diffraction and thermogravimetric analysis show that the compounds with highest transition temperatures have the orthorhombic oxygen defect perovskite structure. The formal valence of Cu and the oxygen stoichiometry factor play an important role in deciding the superconducting behaviour.

Measurements of a.c. susceptibility on unannealed and annealed $La_{2+x}Ba_{4-x}Cu_6O_{14\pm y}$ reveal the presence of a minor superconducting phase in the unannealed compounds.

The thermal expansion of the superconducting compound $YBa_2Cu_3O_7$ has been measured in the temperature range 80K to 235K with a high resolution capacitance dilatometer. There is no detectable change in the thermal expansivity at the critical temperature. The thermodynamic relations associated with the thermal expansion behaviour of $YBa_2Cu_3O_7$ were used to show that the pressure dependence of the critical temperature (dT_c/dp) is smaller than 0.078 K/kbar.

1. GENERAL INTRODUCTION TO SUPERCONDUCTIVITY

In 1911, Kamerlingh Onnes discovered the extraordinary behaviour of certain metals whilst investigating the variation of their electrical resistance with temperature. The d.c. electrical resistivity of these metals falls very close to zero when they are cooled below a critical temperature T_c. The phenomenon was called superconductivity.

Many metallic elements and intermetallic compounds exhibit the superconducting property. The purity, the strain and the metallic properties of a material affect the superconducting transition temperature (M.Tanenbaum and W.V.Wright, 1962). The width of the temperature range over which the resistance drops to zero is much narrower for pure, single crystal specimens than for an impure sample. The zero resistivity of a superconductor leads to the setting up of permanent currents. If a superconducting ring is maintained below its transition temperature T_c, and closed currents are set up by magnetic induction, the current will persist indefinitely without dissipation.

The next important discovery, the Meissner effect was made by Meissner and Ochsenfeld in 1933 while studying the magnetic behaviour of superconductors. They observed that when a bulk superconductor is in a weak magnetic field and then cooled below its critical temperature T_c, magnetic flux is expelled from the interior of the material except for a thin layer at the surface. This phenomenon is called Meissner effect. For a thin specimen, with the long axis parallel to the applied field B_a,

$$B_{int} = B_a + \mu_o M = 0 \qquad (1.1)$$

where B_{int} is the field in the interior of the sample, μ_o is the permeability of the material and M is the magnetization of the specimen.

When the dimensions of the specimen perpendicular to the applied magnetic field are small, the demagnetizing effects can be neglected and there is complete flux expulsion. When the demagnetizing effects are appreciable, the superconducting and normal domains are formed. In the field range $B_c (1-D) < B < B_c$ where D is the demagnetizing factor, the specimen is said to be in the intermediate state.

The above class of materials are referred to as type I superconductors. This behaviour is found in pure elements. When the applied field is below a certain critical value B_c, the surface currents produce a flux which oppose the flux due to the applied magnetic field. Hence, a bulk superconductor behaves like a perfect diamagnet. If the applied field is stronger than the critical field B_c, the superconductivity is destroyed. The critical field B_c is zero at T_c and it increases as the temperature of the specimen decreases. The variation of B_c with temperature T follows a parabolic relation:

$$B_c (T) = B_c (0) \left[1 - \left(\frac{T}{T_c} \right)^2 \right] \qquad (1.2)$$

If the superconductor at a temperature $T < T_c$ carries a current which produces a local field equal to B_c, the superconductivity will be destroyed. This current is referred to as the critical current.

When a thin long superconducting specimen of type II is placed parallel to the applied magnetic field, the magnetic flux is expelled completely until the field reaches a value $B_{c_1} < B_c$ where B_c is the thermodynamic critical field. For $B > B_c$, the flux penetrates the specimen gradually, but the specimen remains superconducting. The superconducting state exists until the field reaches a value B_{c_2}. Above B_{c_2}, there is complete penetration of flux and the superconductivity disappears. B_{c_1} and B_{c_2} are the lower and upper critical fields respectively. Type II is characterized by a vortex state or a mixed state in the field range $B_{c_1} < B_c < B_{c_2}$.

The superconducting state is a thermodynamically reversible equilibrium state. The difference between the free energies of a material in its normal and superconducting states at any temperature T below T_c is given by, (Gorter and Casimire, 1934),

$$f_n(T) - f_s(T) = \frac{1}{2} \frac{B_c^2(T)}{\mu_o} \qquad (1.3)$$

The heat capacity in the superconducting state has an exponential temperature dependence. The superconducting transition in zero field has no latent heat. The specific heat has a discontinuity and the transition is said to be of the second order. The discontinuity in the specific heat is given by

$$c_s - c_n = \left(\frac{T_c}{\mu_o} \right) \left(\frac{dB_c}{dT} \right)^2_{T_c} \qquad (1.4)$$

$c_s - c_n$ is negative at low temperatures and as T tends to zero K, dB_c/dT tends to zero.

In the presence of a field a superconductor releases heat while undergoing a transition from the normal state to the superconducting state. The difference in entropy between the normal and the superconducting states is given by

$$S_n - S_s = - \left(\frac{VB_c}{\mu_o} \right) \left(\frac{dB_c}{dT} \right) \qquad (1.5)$$

where V is the volume of the specimen.

The electromagnetic properties of a superconductor could not be explained by Maxwell's equations alone. However, a phenomenological explanation of the properties was given by F.London and H.London in 1935 by introducing an additional equation of state:

$$-\nabla \times j_s = \left(\frac{n_s e^2}{m} \right) B \qquad (1.6)$$

where j_s = current density of the superconducting current

m = the electron mass

n_s = the density of the superconducting electrons

e = charge of an electron.

According to the theory, the supercurrent is determined by the local magnetic field

$$B = \nabla \times A$$

where **A** is the vector potential of the local magnetic field.

Maxwell's equation along with equation (1.6) leads to

$$\nabla^2 B = \frac{B}{\lambda_L^2} \tag{1.7}$$

where $\lambda_L = \left\{ \frac{m}{\mu_o n_s e^2} \right\}^{1/2}$.

λ_L is called the London penetration depth.

Consider a semi-infinite specimen which extends everywhere for $x<0$. Let B_{ext} be the applied field parallel to the surface in the z-direction. Then at any point $x<0$, the solution of (1.7) yields the field

$$B_z = B_{ext} \exp\left[- x/\lambda_L \right] \tag{1.8}$$

Thus the field decreases exponentially within the superconductor.

The actual penetration depth λ as determined by experiments is greater than the London penetration depth. This may be due to the rigidity of the wavefunction in the superconducting state. The London relation between the current density and the vector potential is a local relation. The variation of the actual penetration depth λ with temperature T is described by the empirical relation,

$$\frac{\lambda(T)}{\lambda(0)} = \left\{ 1 - \left[\frac{T}{T_c} \right]^4 \right\}^{-\frac{1}{2}} \qquad (1.9)$$

The excess penetration depth could be interpreted by introducing the concept of coherence length. Quantitative interpretation was given by A.B.Pippard (1950) who modified the London model. The relation between the current density and the electric field was replaced by a non-local relation. The superconducting state has a long range order. The coherence length is the characteristic length over which the superconducting order persists. It is the range over which the average value of the vector potential A has to be taken to get the current density.

In Pippard's model, the uncertainty principle is used to determine the coherence length ξ_o (Tinkham, 1975). The electrons that are involved in superconductivity are those which lie within an energy $k_B T_c$ of the Fermi surface. These electronic states have a momentum range

$$\Delta p \approx \frac{k_B T_c}{v_F}$$

where v_F is the Fermi velocity and k_B is the Boltzman constant. According to the uncertainty principle,

$$\Delta x \, \Delta p \geq \hbar$$

$$\therefore \Delta x \approx \frac{\hbar v_F}{k_B T_c}$$

Hence,
$$\xi_o \approx \frac{\hbar v_F}{k_B T_c} \qquad (1.10)$$

ξ_o is the distance over which the wavefunction representing the superconducting charge carriers can extend. In pure superconductors like tin and indium, the intrinsic coherence length $\xi_o >> \lambda_L$. The effective number of electrons that contribute to the screening current at the surface decreases by a factor λ/ξ_o.

The actual penetration depth $\lambda = (\lambda_L{}^2 \xi_o)^{1/3}$. The non-local aspects considered in the above treatment are due to the finite extent of the electron mean free path ℓ. In an impure metal, the coherence length decreases and is expressed as

$$\frac{1}{\xi} = \frac{1}{\xi_o} + \frac{1}{\ell} \qquad (1.11)$$

Another phenomenological approach was made by Ginzburg and Landau (1950). The theory is based on Landau's theory of the second order phase transitions. They introduced the concept of the order parameter $\psi(r)$ for the superconducting electrons.

$$n_s = |\psi(r)|^2$$

The supercurrents are described by the phase of the order parameter. The theory accounts for the spatial inhomogeneity of the order parameter present in a superconductor. The free energy of the superconductor depends only on $|\psi|^2$. The theory can be used to explain the condition in which superconductivity and magnetism coexist. The order parameter ψ can be considered as the wavefunction of the centre of mass motion of the Cooper pairs which is introduced in the microscopic theory of superconductivity. It was shown by Gorkov that the Ginzburg-Landau theory is a limiting form of the BCS theory near T_c.

The two characteristic lengths associated with a superconductor are $\xi(T)$ and $\lambda(T)$. $\xi(T)$ is the temperature dependent coherence length and is related to the Pippard coherence length ξ_o. As the impurity content in the material increases, the coherence length ξ decreases (R.P. Huebener, 1979).

$$\text{Near } T_c,\ \xi(T) = 0.740 \frac{\xi_o}{(1-t)^{1/2}} \qquad \text{(pure)}$$

$$\text{and } \xi(T) = 0.855 \frac{(\xi_o \ell)^{1/2}}{(1-t)^{1/2}} \qquad \text{(dirty)}$$

where $t = T/T_c$. (1.12)

Near T_c, the temperature dependent penetration depth

$$\lambda(T) = \frac{\lambda_L(0)}{\sqrt{2}\,(1-t)^{1/2}} \rightarrow \text{(pure)}$$

$$\text{and} \quad \lambda(T) = \frac{\lambda_L(0)}{\sqrt{2}\,(1-t)^{1/2}} \left(\frac{\xi_o}{1.33\ell} \right)^{1/2} \text{(dirty)}$$

$\lambda_L(0)$ = London penetration depth at T=0K. (1.13)

The ratio of the two characteristic lengths is the GL parameter $\kappa = \lambda/\xi$. The parameters λ and ξ are used in determining the wall energy associated with the interface between the normal and the superconducting domains. At the interface, the superconducting behaviour due to the order parameter n_s does not disappear abruptly. It approaches gradually over a distance determined by the coherence length. This results in a decrease in the free energy. The second contribution to the free energy is due to the field penetration into the superconducting phase.

In the intermediate state of type I superconductors, the surface energy is positive. This implies that the surface area between the normal and the superconducting regions is minimized. For $\xi > \lambda$, the wall energy is positive and the materials are classified as type I superconductors. For $\xi < \lambda$, the wall energy is negative and the materials are classified as type II superconductors.

$$\kappa < \frac{1}{\sqrt{2}} \quad \text{for type I superconductors}$$

$$\kappa > \frac{1}{\sqrt{2}} \quad \text{for type II superconductors.}$$

The surface energy associated with the boundary controls the structure of the intermediate state. The structure of the intermediate state depends on the thermodynamic path along which the state of the specimen has been reached. Hence, the intermediate state is a metastable state. This condition is associated with the nucleation and growth of the normal and superconducting phases. The

domain pattern also depends on the thickness of the specimen and its crystalline state. In type II superconductors, the magnetization is generally irreversible.

In the mixed state or the vortex state of type II superconductors, the superconducting currents flow in the vorticies throughout the specimen. The magnetic flux is concentrated at the cores and is quantized. The magnetic flux through each core is given by $\Phi_o \approx \frac{h}{2e}$. It is dispersed through the cores in the form of single flux quanta. When the applied field is B_{C_1}, the magnetic flux through a single core is given by $\Phi_o \approx B_{C_1} \pi\lambda^2$. When the applied field is equal to the upper critical field B_{C_2}, flux through each core is given by $\Phi_o \approx B_{C_2} \pi \xi^2$.

In the intermediate state of type I superconductors, the normal regions contain many flux quanta.

Some information regarding the microscopic nature of the superconductivity was provided by the experiments involving the measurement of specific heat and isotope effect in superconductors. Corak et al (1954) measured the electronic specific heat of vanadium. Specific heat in the superconducting and the normal states were given by

$$C_{es} = \gamma T_c \, a \, e^{-bT_c/T}$$

$$\text{and} \qquad C_{en} = \gamma T. \qquad (1.14)$$

where a and b are constants. γ is the Sommerfeld constant. γ is proportional to the electronic density of states at the Fermi surface. The exponential variation of C_{es} gave evidence for an energy gap for excitation of electrons from the superconducting ground state.

The measurements of the critical magnetic field in mercury isotopes by Maxwell (1950) indicated the dependence of critical temperature on the isotopic mass. The relation between the critical temperature T_c and the isotopic mass M is expressed as

$$T_c M^{\alpha} = \text{constant.} \qquad (1.15)$$

where $\alpha \approx \frac{1}{2}$. The isotope effect suggested that the superconductivity could be due to a strong interaction between the electrons and the lattice.

The next major step was made by Cooper, who showed that if there is a weak effective interaction between a pair of electrons, then such an interaction gives rise to the formation of a bound pair due to the Fermi sea, so that the total energy is less than $2E_F$ where E_F is the Fermi energy. Bardeen, Cooper and Schrieffer showed how Cooper's results could be extended to many interacting electrons. They derived the many body solution of electrons with weak interaction. The Hamiltonian for the system was taken by using the second quantization field operators.

When the centre of mass of two electrons at r_1 and r_2 is at rest, the orbital wave function $\psi(r_1, r_2)$ is of the form

$$\psi_o (r_1 - r_2) = \sum_k g_k \, e^{ik.(r_1 - r_2)} \qquad (1.16)$$

where g_k is the probability of finding an electron with wavevector k and another electron with wavevector -k.

The electrons responsible for the superconducting behaviour are those close to the Fermi surface. Coulomb interaction between the electrons produces a repulsion. A net attractive interaction between the electrons is possible by means of interchange of virtual

phonons (E.A.Lynton, 1962). The ions are distorted in response to a moving electron. A second electron in the vicinity is in turn affected by this phonon.

Consider an electron of wavevector k_1 giving rise to a virtual phonon q which is absorbed by an electron of wavevector k_2. In the process, the electron of wavevector k_1 is scattered into $k_1^1 = k_1 - q$ and the electron of wavevector k_2 is scattered into $k_2^1 = k_2 + q$. The net momentum is conserved, The phonons have a very short life time and the energy may not be conserved. The electron phonon interaction results in an attractive interaction when the energy difference $\Delta\epsilon$ between the electrons involved is less than the phonon energy $\hbar\omega_q$ where ω_q is the frequency of the phonon of wavevector q. Superconductivity occurs only when such an effective attractive interaction between the electrons dominates the repulsive short-range screened Coulomb interaction (Bardeen, Schriefer and Cooper, 1957). The electrons which have such an attractive interaction lie in a region of width $\hbar\omega_q$. All bound pairs have the same total momentum. This interaction between the electrons is cut off when the phonon energy is of the order of Debye energy $\hbar\omega_q = k\theta_D$, beyond which the interaction becomes repulsive. The electrons that follow the above criteria are those having opposite spins and equal and opposite momenta. The pairing of such electrons gives rise to a cooperative many-particle state.

The microscopic theory accounts for the superconducting ground state. The transition from the superconducting to the normal state takes place when an electron pair breaks up into Fermions. This depairing requires a minimum amount of energy, 2Δ. Hence, the lowest excited state is separated from the superconducting state by an energy gap 2Δ.

According to the theory, the ground state energy of the system is expressed as

$$W(0) = - 2 N(0) (\hbar\omega_q)^2 \exp\left[\frac{-2}{N(0)V} \right] \qquad (1.17)$$

where V is the interaction parameter and N(0) is the density of electronic states of one spin direction in the normal metal per unit energy at the Fermi surface. W(0) is also given in terms of the number of electrons n_c, virtually excited above the Fermi level.

$$W(0) = - \frac{n_c^2}{2\,N(0)}$$

The critical temperature at which the superconducting transition occurs is given by

$$k_B\,T_c = 1.13\,\hbar\omega_q \exp\left[- \frac{1}{N(0)V} \right] \qquad (1.18)$$

The energy gap is temperature dependent. At zero temperature the energy gap

$$\Delta(0) = 2\,\hbar\omega_q \exp\left[- \frac{1}{N(0)V} \right] \qquad (1.19)$$

For weak-coupling superconductors, in which $\frac{\hbar\omega_q}{k_B T_c} >> 1$, the variation of Δ with temperature near T_c is given by

$$\frac{\Delta(T)}{\Delta(0)} \approx 1.74 \left(1 - \frac{T}{T_c} \right)^{1/2} \qquad (1.20)$$

In the normal state of a metal, the free electrons get scattered by the lattice and the phase of the electron wavefunction changes rapidly. In the superconducting state, the Cooper pairs are not scattered. The electron pair waves remain coherent. The wavefunction describing the superconducting state is a many particle wavefunction which maintains phase coherence over macroscopic distances. This property of phase coherence is used to explain the flux quantization that is observed in a superconducting ring. Since the wavefunction describing the supercurrent is single valued, the phase changes by an integral multiple of 2π on going once round the closed circuit. The magnetic flux enclosed by the ring is quantized and is given by

$$\Phi = n\left(\frac{h}{2e} \right)$$

where n is an integer.

Another important development made in the study of superconductivity was the discovery of Josephson effect. Supposing there are two superconductors separated by a thin gap of insulating material, the electron pairs can tunnel across the gap. This means that the supercurrent flows across the junction even when there is no potential difference across the junction. The phase coherence will still be present even after the supercurrent crosses the junction. But there will be a phase change $\Delta\phi$ across the junction. The tunnelling current i is given by

$$i = i_0 \sin(\phi_A - \phi_B)$$

where ϕ_A and ϕ_B represent the phases of the wavefunction in the superconductors A and B. i_0 is a constant depending on the effect of the electron-pair coupling across the insulator (Kittel C). It is the maximum current across the junction when there is no potential difference across the junction. This is the d.c. Josephson effect.

If a d.c. potential V is applied across the junction, the tunnel current is an alternating current of frequency $\nu = \frac{2eV}{h}$.

Although a considerable amount of work was done in the past, the highest superconducting transition temperature reported before November 1986 was only 23.2K in Nb_3 Ge (J.R.Gaveler, 1973). In November 1986, Bednorz G.J. and Müller K.A. discovered superconductivity in lanthanum barium copper oxide systems with the onset near 30K. This remarkable discovery inspired the research activity worldwide due to the high temperatures at which superconductivity occurs and its possible applications in technology. Since then many investigations have been done on similar systems. The variation of T_c was studied by replacing barium by strontium and calcium. Strontium substitution raised the T_c to 40K. Subsequently, superconductivity in the 90K range was discovered by Wu

et al (1987) in yttrium barium copper oxide compounds. Superconductivity above the boiling point of liquid nitrogen has been even more exciting and initialized the search for other similar structures exhibiting high temperature superconductivity. These compounds have very interesting structural, electrical and magnetic properties. Tremendous efforts have been focussed towards material processing techniques.

In this work, the superconducting properties of the following oxide ceramics have been investigated:

1. $YBa_2Cu_3O_{7-y}$
2. $La_{2+x}Ba_{4-x}Cu_6O_{14\pm y}$.

2. REVIEW OF HIGH TEMPERATURE SUPERCONDUCTIVITY

a. Introduction

Since the discovery of high temperature superconductivity in lanthanum barium copper oxide systems by Bednorz G J and Müller K A (1986), a great deal of experimental and theoretical work has been done. Several groups have concentrated on characterizing the new copper oxide based superconductors and understanding the mechanism involved in high temperature superconductivity. The superconducting oxides studied so far have been classified into two categories.

1. $(La_{1-x}, Sr_x)_2CuO_{4-y}$ of the body centred tetragonal K_2NiF_4 type having T_c in the range 30-40K.
2. $YBa_2Cu_3O_{9-y}$ of the oxygen deficient perovskite (ODP) type having T_c around 90K.

In this chapter, the results of the investigations of crystal structure, magnetic, electrical and thermal properties of these compounds by several research groups have been briefly reported.

Superconducting metallic oxides have been known since 1973 (David Johnston). Perovskite like structures $LiTi_2O_4$, $SrTi_2O_3$ and $Ba(Pb_{1-x},Bi_x)O_3$ have shown the superconducting behaviour. The superconducting transition temperature never exceeded 15K in these compounds. Bednorz and Müller concentrated on oxides having high electron phonon coupling and also having a tendency for polaron formation. They investigated the properties of $Ba_xLa_{2-x}Cu_5O_{5(3-y)}$ for x=1,0.75 and y > 0. This is a mixed phase system in which the conduction electron states lie between the non Jahn Teller Cu^{3+} and the Jahn Teller Cu^{2+} ions. The lattice deformation caused by the Jahn Teller effect for Cu^{2+} can give rise to polaron formation. A phase transition between the superconducting and bipolaronic insulating states is possible in such a system.

Bednorz and Müller prepared $Ba_xLa_{5-x}Cu_5O_{5(3-y)}$ by a co-precipitation method. They mixed the aqueous solutions of nitrates of barium, lanthanum and copper in the appropriate ratio. The mixture was then added to an aqueous solution of oxalic acid.

The solid precipitate was heated at 900°C for five hours and pressed into pellets at 4 kbar and then sintered at 900°C. The sample prepared was granular and porous.

The resistivity measurements of $Ba_xLa_{5-x}Cu_5O_{5(3-y)}$ with $x \leq 1$ in the temperature range 300K to 4.2K showed that as the sample was cooled from room temperature, the resistivity first decreased and at low temperatures increased logarithmically. On further decrease of temperature, a sharp drop in resistivity was observed. The data indicated the onset of superconductivity at 30K and zero resistivity below 13K. The X-ray diffraction lines showed that the compound was a mixture of three individual phases $La_{1-x}Ba_xCuO_{3-y}$ with a perovskite structure, $La_{2-x}Ba_xCuO_{4-y}$ with a layered perovskite structure of K_2NiF_4 type and CuO. The relative volume of these phases in a compound depends on heat treatment. The volume fraction of the sample that was superconducting could be determined by measuring the magnetic susceptibility of the sample in the superconducting state and could be related to the intensities of the lines in the X-ray diffraction pattern. Hence, the composition and structure of the superconducting phase could be identified. There was a clear indication of superconductivity occurring in one phase of $Ba_xLa_{5-x}Cu_5O_{5(3-y)}$. Since the sample was polycrystalline and had different crystalline phases, the superconductivity was of a percolative nature.

Recently, many groups have prepared the superconducting compounds by the direct oxide technique. A single phase of the compound $Ba_xLa_{2-x}CuO_{4-y}$ prepared by this technique exhibits superconductivity below 23K. It is superconducting for values of x=0.05, 0.10 and 0.15. The sample is prepared by taking La_2O_3, CuO and $BaCO_3$ powders and mixing them in appropriate cation ratio. The mixture is heated in air or oxygen for several hours. The resulting compound is then cooled, ground and then pressed into pellets and sintered at 900°C to 1100°C. The superconducting phase in this compound is related to the single layered like K_2NiF_4 structure (Takagi H et al 1987a).

An increase in T_c is observed in this system due to the effect of pressure. When the pressure increases, T_c increases at a rate of 10^{-3} K/bar. A pressure of approximately 13.3 kbar raises the onset of superconductivity to 40.2K (Chu C.W. et al 1987).

When barium is replaced by the alkaline earths Sr or Ca, the sample is still found to be superconducting. The replacement of Ba by Ca decreases the T_c to 18K. Sr substitution enhances the transition temperature to 48.6K and the transition width is approximately 2K (R.J.Cava et al, 1987a).

When lanthanum is replaced by yttrium, the onset of superconductivity occurs at 93K in $Y_{1.8}Ba_{0.2}CuO_{4-y}$ (Wu et al). $Y_{1.8}Ba_{0.8}CuO_{4-y}$ has multiple phases which are different from the K_2NiF_4 type. Superconductivity in this system could be due to interfacial interaction between phases. The system has two different phases Y_2BaCuO_5 (green) and $YBa_2Cu_3O_{9-y}$ (black) with $y=2.1 \pm 0.05$. The latter phase is superconducting while the former is not superconducting. $YBa_2Cu_3O_{9-y}$ is a distorted oxygen deficient perovskite. In contrast to $La_{2-x}Ba_xCuO_{4-y}$, pressure has little effect on the T_c of $Y_{1.2}Ba_{0.8}CuO_{4-y}$ (Hor PH et al 1987a).

A single phase of the Y-Ba-Cu-O compound is prepared by the high temperature solid state reaction of the oxides of Y, Ba and Cu. (R.J.Cava et al, 1987b). A mixture of high purity Y_2O_3, $BaCO_3$ and CuO powders is ground and calcined in air at 950°C for 24 hours. The calcined material is again ground to get a homogeneous compound and then pressed into pellets. It is then sintered in flowing oxygen for 16 hours and cooled very slowly to 200°C in the same atmosphere. Further sintering in oxygen at 700°C results in a better superconducting material.

Better processing techniques have led to the preparation of single phase compounds with a sharp superconducting transition. In these ceramics it is the structure that controls the superconductivity. Oxygen content depends on the cooling rate, firing temperature and the atmosphere in which the samples are

sintered. The orthorhombic to tetragonal structural phase transition that is observed depends on the oxygen content. The index y in the formula denotes the non-stoichiometry. It represents the average of the fraction of the oxygen vacancies in the unit cell. A specimen annealed under a nitrogen or argon atmosphere has poor superconducting properties because of a low oxidation state. To determine the oxygen content, thermogravimetric data is obtained by taking the weight changes in oxygen while annealing the specimen. The observed weight change can be converted to stoichiometry. The factor y depends on the partial pressure of oxygen and the temperature at which the sample is sintered. Since the phase of the compound which is responsible for superconductivity has to establish equilibrium with oxygen, slow cooling is necessary. Rapid cooling results in a highly disordered state. Perovskite structure may be conserved but barium and yttrium exhibit a high degree of disorder. Quenching conditions are important in the preparation of a homogeneous compound.

Most of the experimental data have been taken on polycrystalline materials. The anisotropic behaviour of the physical properties can be investigated in greater detail from experiments with single crystal specimens. Recently, some groups have reported the growth of single crystals of $YBa_2Cu_3O_{9-y}$. The phase diagram representing the ternary system illustrates the region of partial melting (Fig.2.1, Roth et al, 1987). Flux required for crystal growth is obtained from the region (D) and heated to 800^oC for more than 4 hours and then to 1000^oC at a rate of 50^oC/hr. The specimen is retained at this temperature for three to five hours and then cooled below 880^oC at a rate of 4 to 15^oC/hr. (L.F.Scheemeyer et al, 1987). The crystals formed are bulk superconductors.

Several other methods are being employed to prepare the cuprate superconductors. The plasma oxidation technique yields a compound rich in oxygen content compared to the heat treatment. The oxidation takes place at $\leq 80^oC$. This method has been used to induce

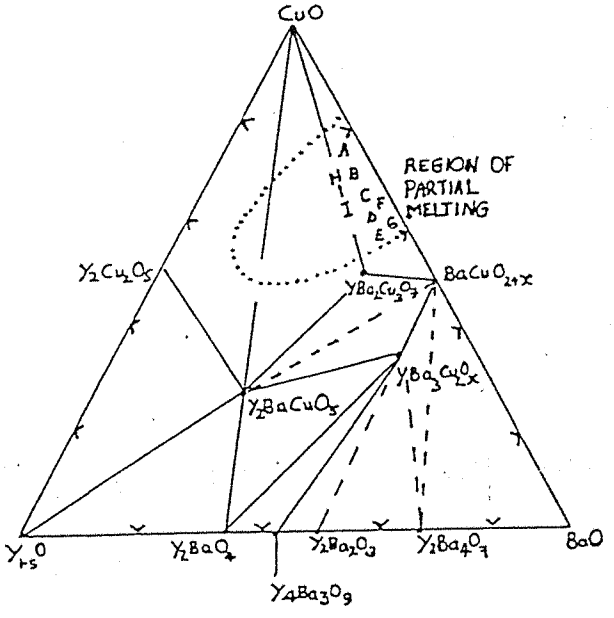

Figure 2.1. BaO-CuO-Y_2O_3 Ternary Phase Diagram ($\sim$950-1,000°C). (Roth et al 1987).

superconductivity in non-superconducting compounds. Attempts have been made to produce homogeneous compounds by the citrate gel process. Thin films have been prepared by sputtering techniques.

b. Superconductivity in $La_{2-x}(Ba/Sr)_xCuO_{4-y}$ (K_2NiF_4 type) compounds

Structure of La_2CuO_4

The high temperature superconductors with the composition $La_{2-x}Ba_xCuO_{4-y}$ are derived from the parent compound La_2CuO_4. The structure of La_2CuO_4 and La-Ba-Cu-O compounds is based on the Perovskite structure with the formula ABX_3 (Galasso F.S., 1970). A perovskite has a cubic structure, with A atoms at the centre having a coordination of 12 X atoms and B atoms at the corners having a coordination of 6 X atoms arranged octahedrally. This is referred to as A unit. The B unit consists of B atom at the centre, A atoms at the corners and X atoms at the centre of each face. The La_2CuO_4 structure is obtained by taking one B unit and two A units (without one BX_3 layer) and arranged as shown in Fig.2.2. The La atoms have a coordination of only 9 oxygen ions. The perovskite layers consist of corner sharing CuO_6 octahedra. The structure of La_2CuO_4 is of K_2NiF_4 type. It is orthorhombic at room temperature and changes into the tetragonal form at 533K.

All the Cu ions are divalent in this compound. The structural transition temperature of La_2CuO_{4-y} increases rapidly from 450K to 530K as y increases from 0 to 0.1.

The transport behaviour of lanthanum copper oxide is very much affected by the stoichiometry of the compound. (Singh et al, 1984). The preparation conditions have been found to affect the properties of La_2CuO_4. The transport behaviour is partly dependent on the sintering temperature as well as the duration of heat treatment. When the compound is annealed in oxygen at high pressure a mixed valence state of Cu is formed and the compound is superconducting. The La deficient La_2CuO_4 is found to be superconducting below 35K (P.M.Grant et al, 1987). The magnetic

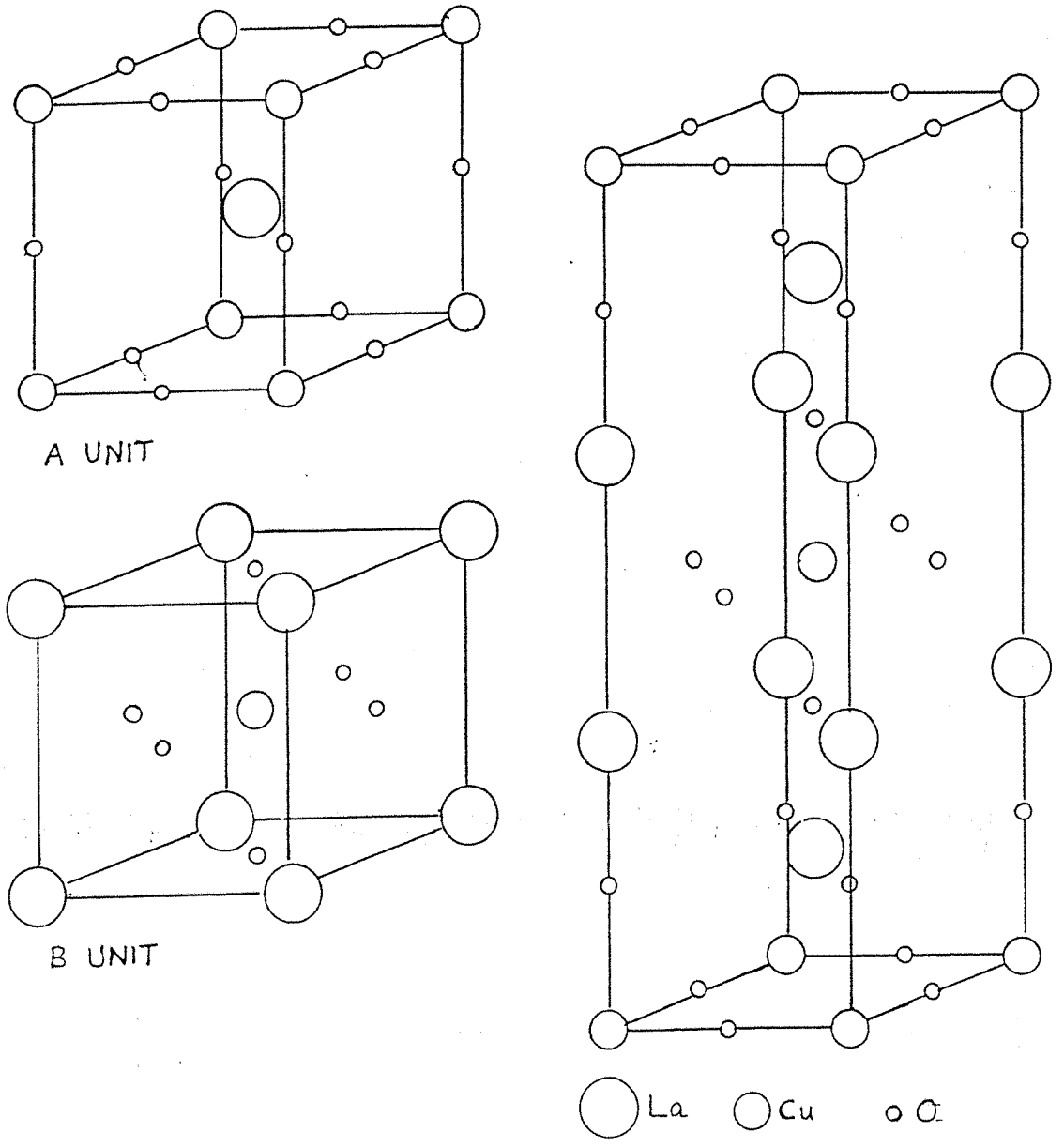

Figure 2.2. The crystal structure of La_2CuO_4.

susceptibility of La_2CuO_4 shows an anomaly (cusp) at 220K and indicates an antiferromagnetic transition at 220K (Nishihira et al, 1987). The magnetic susceptibility data obtained by Bednorz and Müller (1987a) in the temperature range 4K to 300K shows a weak paramagnetic behaviour at high temperatures and an anomaly (cusp) at 250K. On further decrease of temperature, there is an increase in susceptibility below 50K and the magnitude of the susceptibility is field dependent. When the temperature of the compound falls below 35K, there is a small diamagnetic contribution to the susceptibility and its magnitude depends on the zero field or field cooled conditions in which the measurements are made. The resistivity of the sample increases logarithmically at low temperatures and a peak occurs near 50K. This increase in resistivity at 50K suggests that the charge carriers are localized. The Curie-like behaviour in magnetic susceptibility observed below 50K may be due to the contribution from the localized spins. Below 35K, the superconductivity is established in alkaline earth doped La_2CuO_4. This implies that either a small part or the whole of the undoped compound is superconducting. This is in accordance with the fact that the oxygen excess or deficiency of lanthanum change the valency of copper in the same manner as found in alkaline earth doped La_2CuO_4.

The Curie-Weiss-like behaviour above the cusp at 250K shows an antiferromagnetic ordering with θ=250K. The value of the estimated Curie constant corresponds to an effective magnetic moment 0.5 μ_B. If the magnetic moments are due to the spins of electrons from the copper 3d states, then the magnetic moment corresponds only to a very small percentage (9.1%) of the spins localized on Cu^{2+}. Hence, there is a possibility of a spin density wave giving rise to the observed magnetic behaviour.

Stoichiometric substitution of group II elements in La_2CuO_4 led to the new superconductors represented by the formula $(La_{1-x}A_x)CuO_4$ where A=Ba,Sr or Ca. These superconducting oxides have a tetragonal K_2NiF_4 type structure at room temperature. Barium or strontium occupy the La sites. Each kind of cation gives rise to a

planar sheet. The alkaline earth substitution causes volume changes and results in distortions of the Cu site. The Cu-O distance in the perovskite layer is less than the Cu-O distance normal to the perovskite layer. The copper ions are linked to each other by oxygen ions. There are alternate layers of perovskite (CuO_3) and rock salt La(Sr)O structures.

The distance between the CuO_2 planes is greater than 6Å. The band structure calculations show that weak interactions exist between CuO and La atoms. Although there is significant charge transfer from La atoms, their contribution to the conduction bands is negligible (A.J.Freeman et al, 1987). Each Cu ion in the CuO_6 octahedron has a tight binding within each layer. A Cu^{2+} ion has a configuration $3d^9$. The five d orbitals in a octahedron of O_6^{2-} split into a doublet e_g and a triplet t_{2g}. The orbitals of lower energy correspond to t_{2g}. When the orbitals of higher energy are not symmetrically occupied, the regular octahedron is elongated along the c-direction (Jahn-Teller effect) and gives rise to a stable configuration. In $(La_{1-x}Sr_x)_2CuO_{4-y}$, as x increases, the ratio of the lattice parameters c_o/a_o increases giving rise to further elongation of the octahedra (Kishio K et al, 1987b).

$(La_{0.925}Ca_{0.075})_2\ CuO_{4-y}$ has a $T_c \approx 18K$. Sr substitution increases the T_c to 36K (Kishio K et al 1987a). The compounds $La_{2-x}(Sr,Ba)_xCuO_{4-y}$ are superconducting only when the value of x lies in a certain range. For $x < 0.04$ or $x > 0.3$, the compound is semiconducting. The resistivity of samples which are as quenched in air shows a semiconducting behaviour and the samples annealed in oxygen show a superconducting behaviour. Hence, T_c depends on the concentration of La and Ba/Sr and also on the heat treatment. The superconducting transition is obtained for the composition where an orthorhombic to tetragonal structural phase transition takes place. Highest T_c is obtained when the material is just short of transition to orthorhombic symmetry. As the lattice parameter a_o decreases, the transition temperature increases.

The high temperature tetragonal K_2NiF_4 phase of La_2CuO_4 is stabilized when the compound is doped by Sr^{2+} or Ba^{2+}. This results in the formation of Cu^{3+} ions. Thus the charges are neutralized. Any change in the concentration of Ba and La changes the Cu^{2+}:Cu^{3+} ratio. The formal valence of Cu in $(La_{1-x}Ba_x)_2CuO_4$ is 2.15. Annealing the compound in a reduced atmosphere may bring the Cu^{3+} back to Cu^{2+} and the superconductivity is destroyed. Thus a mixed valence state seems to play an essential role. T_c increases as Ba concentration increases and the superconductivity is destroyed when the ratio Cu^{3+}:Cu^{2+} reaches a certain maximum.

High pressure on $(La_{1-x}Ba_x)_2CuO_{4-y}$ enhances its superconducting transition temperature. This suggests that T_c is related to the Cu-O distance in the Perovskite layer and the overlap of the Cu d and oxygen p orbitals in the CuO_2 layer.

A study of lattice dynamics is very necessary to determine the existence of electron-phonon coupling. The investigation of phonon dispersion in $La_{1.85}Ba_{0.15}CuO_4$ by inelastic neutron scattering experiments shows that there is a strong coupling between the conduction electrons and the lattice vibrations associated with the oxygen atoms (G.Balakrishnan et al, 1987). The isotope effect observed in $La_{1.85}Sr_{0.15}CuO_4$ yields a value of $\alpha = 0.16 \pm 0.02$ (Batlogg et al, 1987).

The Cu^{2+} ions in La_2CuO_4 are in an S=½ state (Rao C.N.R. et al, 1984). The conduction bands are formed in the copper oxygen octahedron layers due to the strong hybridization of Cu 3d and O 2p orbitals. According to A.J.Freeman et al (1987a), the orthorhombic phase of La_2cuO_4 results from a strong Fermi surface $|q| = 2k_F$ instability along the [110] direction. Substitution of Ba/Sr changes the carrier concentration and lowers the Fermi energy. When the Fermi energy is lowered, the instability due to the nesting of the Fermi surface is removed and the compound is transformed to a tetragonal phase. The orthorhombic structure is seen upto Sr concentration given by x=0.007. Sr substitution intensifies the

electron phonon coupling constant λ and results in a large value of T_c. If the Sr content exceeds a certain limit, the increase in λ introduces the lattice instability at x=0.125.

Since Sr-O bond is more ionic in character than the La-O bond, Sr substitution leads to a change in the effective charge on O ions. This might result in an enhancement of the crystal field around the Cu ions and can lead to further distortion.

In La_2CuO_4 and La_2CuO_4:Ba, the magnetic susceptibility is field dependent below the transition temperature. A superconducting glassy state has been identified in La_2CuO_4:Ba from measurements of magnetic susceptibility in zero field and field cooled states. The diamagnetism of the specimen is greater in the zero field cooled state than in the field cooled state. When the specimen is cooled in zero field and then a field is applied, the variation of magnetic susceptibility with temperature shows that the magnetic response is reversible with respect to temperature beyond the temperature T^* corresponding to the non-ergodic limit. (Müller K A et al,1987b). T^* is below the temperature corresponding to the onset of superconductivity. For a given value of the applied field H, T^* is specified. The relation between the magnetic field and T^* is in agreement with the Sherrington-Kirkpatrick spin glass model with infinite range interaction.

In the superconducting glassy state, if the field is switched off, a positive remanent magnetization is observed and indicates flux trapping. This behaviour is observed in inhomogeneous type II superconductors. If the temperature of the specimen is increased the magnetization decreases almost linearly and then disappears when the temperature T^* is reached.

The magnetic susceptibility of $La_{2-x}Sr_xCuO_4$ above T_c shows a paramagnetic behaviour and is independent of the magnetic field. The estimated value of the upper critical field at zero K is 47T. The susceptibility is also found to vary with the oxygen content of the compound. The magnetization behaviour is found to be reversible

with respect to temperature only for x=0.10 and 0.15 but not for x=0.2. As the value of x increases from 0.1 to 0.2, the estimated electron density of states is high compared to the value expected from band structure calculations. (Bednorz and Müller, 1987a).

Magnetic hysteresis in the superconducting state, has also been observed in $La_{1.85}Sr_{0.15}CuO_4$ at B < 4mT. The shielding magnetization increases linearly as B increases. When the flux penetrates the specimen, deviation from this behaviour is observed.

A number of new models have been proposed to explain the magnetic behaviour and the high T_c superconductivity. The majority of charge carriers are hole-like in the normal state. If the Jahn-Teller stabilization energy is equal to the bandwidth in a metal, polarons are formed. The effective mass of the conduction electrons or holes gets enhanced and results in a large electron-phonon coupling (Hock et al).

Strong interelectronic repulsive forces in La_2CuO_4 are responsible for the magnetism observed in La_2CuO_4 (Anderson D, 1987). Hence, it may not be possible to explain the high temperature superconductivity behaviour by the conventional B.C.S pairing. The Coulomb interaction between the d electrons may be effectively screened through the strong coupling of the 3d electrons to the lattice and result in an effective attractive interaction and the formation of intersite bipolarons. The interaction of the d electrons with the oxygen p orbitals and the overlap of the nearest neighbours leads to hopping of the conduction electrons and during the process the valence of the neighbouring ion changes to Cu^{3+}. Bipolarons in the insulating state at room temperature may get condensed to charged pairs with strong coupling in the superconducting state. The substitution of Sr or Ba might change the concentration of bipolarons.

c. Superconductivity in $YBa_2Cu_3O_{9-y}$ (ODP type) compounds

The superconductors with high T_c around 90K are grouped under the class $YBa_2Cu_3O_{9-y}$. $YBa_2Cu_3O_{9-y}$ is identified as a pure phase. This is an orthorhombically distorted, oxygen deficient perovskite (ODP). The structure of this compound as obtained from neutron diffraction data is shown in Fig.2.3 (F Beech et al, 1987).

The crystal structure of $YBa_2Cu_3O_7$ is obtained from the ideal perovskite structure by the formation of ordered oxygen vacancies. The structure of $YBa_2Cu_3O_9$ consists of alternating CuO_2 - (Ba,Y)O planes normal to the c-axis. The CuO_6 octahedra form a 3-dimensional cubic lattice. Ba and Y vary in size and so they do not occupy the same lattice points as the divalent and trivalent ions in the K_2NiF_4 structure.

When a unit cell of $YBa_2Cu_3O_9$ is transformed into $YBa_2Cu_3O_8$, the oxygen atoms on the plane containing the Y atoms are missing so that Cu(2) atom is surrounded by five oxygen atoms forming a square pyramid. When the unit cell of $YBa_2Cu_3O_8$ is transformed into $YBa_2Cu_3O_7$, the oxygen vacancies are formed on the same level as the Cu(1) ions in the octahedral layers in between the Ba layers. Cu(1) is surrounded by two O(1) and two O(4) atoms at distances 1.94 Å and 1.846Å respectively. A chain consisting of these CuO_4 units runs along the b-axis. The Cu(2) atom is surrounded by four oxygen atoms (two O(2) and two O(3)) which are almost coplanar. The Cu(2) atom is situated above this plane by $\approx$ 0.28Å .

In the stoichiometric composition, barium has a coordination of ten oxygen atoms. Yttrium is coordinated to a polyhedron of oxygen atoms.

When $y \approx 2.0$, all the O(4) sites are occupied.

When $y \approx 2.2$, 20% of the O(4) sites are vacant on the b-axis.

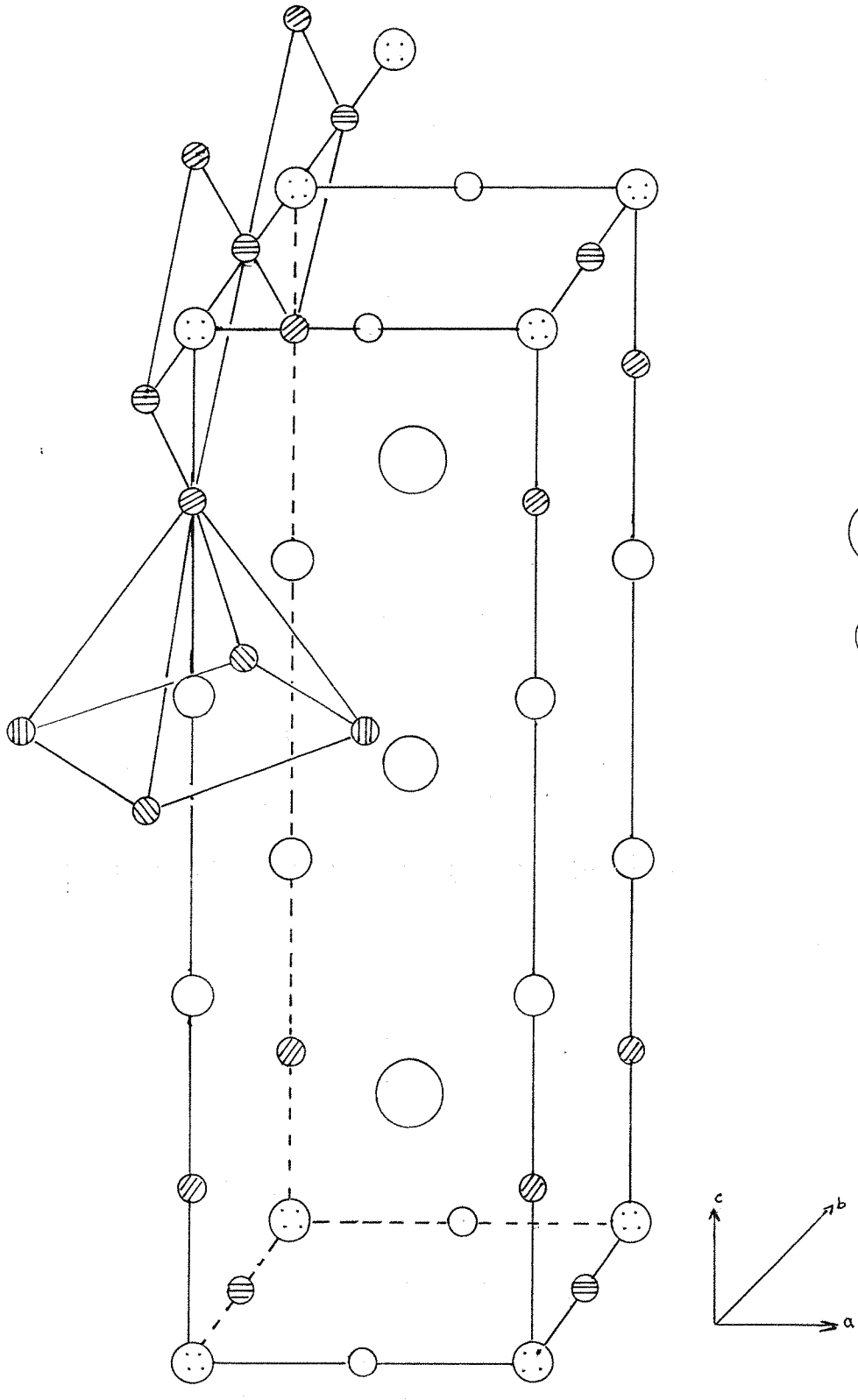

Figure 2.3. The Crystal Structure of $YBa_2Cu_3O_7$

O(5) is a Vacancy.

$YBa_2Cu_3O_7$ gradually loses all the O(4) atoms in transforming to $YBa_2cu_3O_6$ resulting in O-Cu-O linear bonds. $YBa_2Cu_3O_6$ is a semi-conducting compound. Thus we find that the chains of CuO_4 units play an important role in the superconducting mechanism.

In $YBa_2Cu_3O_6$, the Cu(1) and Cu(2) sites are occupied by Cu^{1+} and Cu^{2+} respectively and Cu(1)-O(1) bond length is less than that in $YBa_2Cu_3O_7$ (P.Bordet et al, 1987). For $y > 2.4$, the tetragonal structure results from an ordering of Y and Ba cations and oxygen vacancies.

Annealing in oxygen raises the onset temperature for superconductivity and sharpens the transition. $YBa_2Cu_3O_{9-y}$ is superconducting and the T_c increases from 58K to 92K as y decreases from 2.4 to 2.0. The structure has an orthorhombic symmetry for $2 \leqslant y < 2.4$. The change in T_c depends on the oxygen deficiency.

High T_c superconductivity is attributed to the two dimensional CuO_2-Ba-CuO_{2+x} layers. The basic units are formed by square pyramidal network due to $^2/_3$ of Cu atoms and the planar units due to the remaining $^1/_3$ of Cu atoms. The stability of square planar and square pyramidal Cu coordination is responsible for accommodating a flexible arrangement of oxygen ions in the perovskite structure. Formal valence of Cu is +2.27. Yttrium layers divide the structure into two isolated sheets and a two-dimensional network is created. The barium and yttrium cation layers are ordered according to the repeated sequence Ba-Y-Ba-Ba-Y. Cu^{2+} and Cu^{3+} occupy the square pyramidal and square planar sites respectively.

The difference between the distorted ODP structure and the K_2NiF_4 type structure is that the ODP structure does not have the rock salt layers. The similarity seen in both structures is the presence of two-dimensional copper-oxygen planes.

In the orthorhombic crystal, the Cu-O vibrational modes are evident from Raman scattering data. The Cu(2)-O-Cu(1) bond is stretched along the c-axis and has a frequency of 500 cm^{-1}. In the

tetragonal structure, the frequency of this mode reduces to 470 cm^{-1}. The bonding forces between Cu and O atoms are stronger than the other bonds. The lattice parameter c decreases in the orthorhombic structure. The Cu(2)-O-Cu(1) bond length in the orthorhombic structure is shorter than that in the tetragonal structure. Thus the observed high frequency modes in the orthorhombic structure can be explained (A Yamanaka et al, 1987).

The isotope effect observed in $YBa_2Cu_3O_{9-y}$ shows that the transition temperature decreases by 0.3 to 0.5K when 90% of ^{16}O is replaced by ^{18}O. If the values of α is assumed as $\approx$ 0.5 as in the conventional superconductors, T_c is lowered by 5K when O_{16} is completely substituted by ^{18}O. Thus there is an indication of the presence of electron phonon interaction (Leary et al, 1987).

Both $YBa_2Cu_3O_7$ and $La_{1.85}$ $(Sr,Ba)_{0.5}$ CuO_4 have specific heats which vary linearly with temperature and show an anomaly at T_c. Takagi et al consider a weak-coupling limit for La-Sr-Cu-O. By assuming the BCS relation to hold good they have estimated the electronic specific heat coefficient γ to be 15mJ/mol/K^2 and 11mJ/mol/K^2 in $YBa_2Cu_3O_7$ and $La_{1.85}(Sr,Ca)_{0.15}CuO_4$ respectively (H.Takagi et al, 1987). The tunnelling experiments on $YBa_2Cu_3O_7$ have resulted in an energy gap with a temperature dependence in agreement with the BCS theory. The data show that $YBa_2Cu_3O_7$ is a strong coupling superconductor.

The changes in the electronic energy of the $YBa_2Cu_3O_{7-y}$ system could give rise to the orthorhombic to tetragonal phase transition and change the T_c. The band structure calculations of A.J.Freeman et al (1987b) show that the density of states decreases by 20% as the stoichiometry decreases from 7 to 6.5.

According to the single cell model, the electronic density of states near the Fermi energy arises from the interaction between $Cu(3d_{x^2-y^2})$ and $O(2p_{xy})$ orbitals in the Cu-O square planar layers

which has a two dimensional character. According to the double cell model, the electronic density of states results from the one dimensional chains (Matheiss, 1987). Since the superconducting transition temperature T_c depends on the factor y, the 2D square planar layer or one dimensional CuO_4 chains or both may contribute to the transport properties. The electronic interactions might be significant between the one dimensional chains and the Cu-O planes as they are linked by the O(1) ions.

Since the oxide materials are porous with grain size approximately a few microns, coupled Josephson junctions can exist in the superconducting state. The application of microwave radiation on Y-Ba-Cu-O / Y-Ba-Cu-O Josephson junctions induce distinctive current steps in the current-voltage characteristics. The currents flow when there is resonance in the oscillatory Josephson current with the microwave radiation and are observed at consecutive voltage steps given by (h/2e)f where f is the frequency of the microwave radiation. Thus the onset of macroscopic quantum state below T_c implies the wave nature of the condensed pairs.

The shielding currents are set up in a superconductor in the presence of a time dependent magnetic field in accordance with the law of induction. This results in the flux motion due to the Lorentz force. If the pinning forces are stronger than the Lorentz force, the magnetic field propagation is disrupted and disturbs the thermodynamic equilibrium. This results in a hysteresis behaviour of the magnetization. Flux pinning might occur due to the interaction between the grain boundaries and the fluxoids. In polycrystalline materials, the planar defects are responsible for scattering the charge carriers. Grain boundaries and the planar faults act as pinning centres. In the new copper oxide superconductors, the planar defects are associated with the formation of twin boundaries and extrinsic planar defects. The strength of the pinning force of an imperfect grain boundary is much greater than that of a perfect boundary. In polycrystalline materials of type II

superconductors the critical current is found to be inversely proportional to the grain size (Welch D O, 1985). The grain boundary effects are also seen in the perturbation of the G-L parameter κ.

In powdered samples of $YBa_2Cu_3O_{7-y}$, the behaviour of magnetization M with respect to the applied field B is reversible in low fields (Schauer W et al 1987). Critical current densities of 10^6 A/cm^2 at 1T are observed at 4.2K in the grains. In the bulk samples the critical current densities are very much less than those deduced for single grains in powdered samples. This could be due to the weak link between the individual grains in the bulk samples. The critical current density depends on the microstructure of the material. The intrinsic property of the grains is also revealed in the measurement of the imaginary part of the a.c. susceptibility. The losses are more in the bulk samples compared to that in powdered samples.

The onset of superconductivity in $Y_{1.8}Ba_{0.2}CuO_{4-y}$ is at 92K. This compound when cooled in zero field or high field (B > 90 G) is diamagnetic below T_c. However, when cooled in a field $\leqslant$ 85 G, unusual spurious effects have been observed below T_c in this multiphase compound (Hor et al, 1987).

For both the single phase samples $YBa_2Cu_3O_7$ and $La_{1.8}Sr_{0.15}CuO_4$ the Meissner signals are much smaller compared to the shielding signals obtained after zero field cooling. The magnetic susceptibility of $YBa_2Cu_3O_{9-y}$ above T_c is described by Curie-Weiss law. The Curie constant yields p_{eff} = 0.3 μ_B/Cu atom.

The magnetic properties investigated so far agree with the phenomenological Ginzburg-Landau theory. The estimated value of coherence length $\xi \approx 22$ Å (R.J.Cava et al, 1987b). The variation of the lower critical field B_{c_1} with T is linear in the temperature range 20K - 90K (H.Spille et al, 1987).

The onset of transition as obtained by a.c. susceptibility measurements occurs almost at the same temperature as obtained from resistivity data. But the broadening of the transition is quite large compared to the resistive transition. This could be due to the anisotropic behaviour of B_{c_2} which is not apparent in the resistive transitions.

Anisotropic upper critical fields investigated using preferentially oriented pellets are given by the relation $H_{c_2}(\theta) = H_{c_{2\perp}} (\cos^2\theta + \varepsilon^2 \sin^2\theta)^{-\frac{1}{2}}$ for all the grains. θ is the angle between the c-axis and the magnetic field. $H_{c_{2\perp}}$ and $H_{c_{2\parallel}}$ are the magnetic fields normal and parallel to the crystal layer respectively. ε is the anisotropy factor $H_{c_{2\perp}}/H_{c_{2\parallel}}$ (Takita K et al 1987).

When yttrium is replaced by the trivalent rare earths, all the compounds (except A=Lu), have the $YBa_2Cu_3O_{6+y}$ structure. A superconducting phase with T_c in the 90K range (90-98K) is obtained with the exception of Ce,Pr and Tb. Above T_c, the variation of susceptibility with temperature shows a Curie-Weiss behaviour and the Curie temperatures are negative implying that the rare earth ions have an antiferromagnetic interaction (P.A.J. de Groot et al, 1987). Crystal field effects are significant on the rare earth ion sites as seen from inelastic neutron scattering results (B.D.Rainford, 1987).

The magnetization data suggests the coexistence of magnetic order and superconductivity in the R-123 compounds. There is little overlap of the RE electrons and the electrons responsible for superconductivity. Magnetic hysteresis is observed in these compounds at low temperatures and high fields. When the field is switched off the remanence is large at low temperatures and suggests that the flux pinning still exists. These observations at low temperatures and high fields are in favour of a superconducting glassy state. The estimated value of critical current is

$(2.5 \pm 1) \times 10^5$ amps/cm^2 from hysteresis curves (analysed with critical state model). Since most of the rare earth sites are magnetic, the rare earth sites might act as pinning centres and enhance the value of the critical current j_c. The Curie constant provides p_{eff} consistent with the 4f configuration of the corresponding rare earth ion. The presence of magnetic ions in conventional superconductors almost always reduces T_c.

Since the T_c of $YBa_2Cu_3O_7$ (1-2-3 compounds) is much higher compared to that of $La_{2-x}Ba_xCuO_{4-y}$ compounds, the coupling between the Cu and O atoms in the square planar chains play an important role.

Mössbauer measurements on $GdBa_2Cu_3O_{7-y}$ yield isomer shifts corresponding to insulating Gd-transition metal oxides. Thus the conduction electron density is very low at Gd sites and there is little RKKY interaction (H A Smit et al, 1987).

The symmetry of the compound results in two parallel and antiparallel nearest Gd atoms for Cu in a layer. This leads to the balancing of interactions whatever the type of interactions that are present. This fact might account for the coexistence of magnetic ordering and superconductivity.

Specific heat measurements on $RBa_2Cu_3O_7$ compounds show an anomaly at low temperatures (Ramirez et al, 1987). The temperature corresponding to the ordering of the local moments is much greater than the dipolar energy. Thus exchange interaction is the major interaction that is present. The specific heat data on $DyBa_2Cu_3O_7$ in the presence of a field greater than B_{c_1} indicates that the ordering temperature decreases as the field increases. This observation implies an antiferromagnetic ordering. The antiferromagnetic ordering has also been shown by neutron diffraction results (D Mck.Paul).

The maximum superconducting transition temperature in the La-Ba-Cu-O system was confined to 35-40 K range. Mitzi D.B. et al (1987) succeeded in increasing the transition temperature beyond 70K in $Ba_{1.75}La_{1.25}Cu_3O_{7+y}$. The oxide with the composition $La_3Ba_3Cu_6O_{14+y}$ was investigated before the discovery of the copper oxide superconductors (Er-Rakho et al, 1981). The rate at which oxygen is intercalated has an appreciable effect on its transport properties. The structure of $La_3Ba_3Cu_6O_{14+y}$ is isomorphous with the tetragonal structure of $YBa_2Cu_3O_{7-y}$ (David W I F et al, 1987). Although this is a mixed valence system in two dimensions, the compound exhibits a pure semi-conducting behaviour. Barium and lanthanum ions being similar in size , they mix on the A atom site of the perovskite structure and a solid solution is obtained with the composition $Ba_{2-x}La_{1+x}Cu_3O_{7\pm y}$ for $0 \leqslant x \leqslant 0.5$. The partial phase equilibria of the oxides formed in the $(Ba/La/Y)CuO_{3-y}$ system is as shown in Fig.2.4 (after Cava et al 1987). It is interesting to note that the high T_c in La-Ba-Cu-O system is identified with the $La_{3-x}Ba_{3+x}Cu_6O_{14\pm y}$ phase.

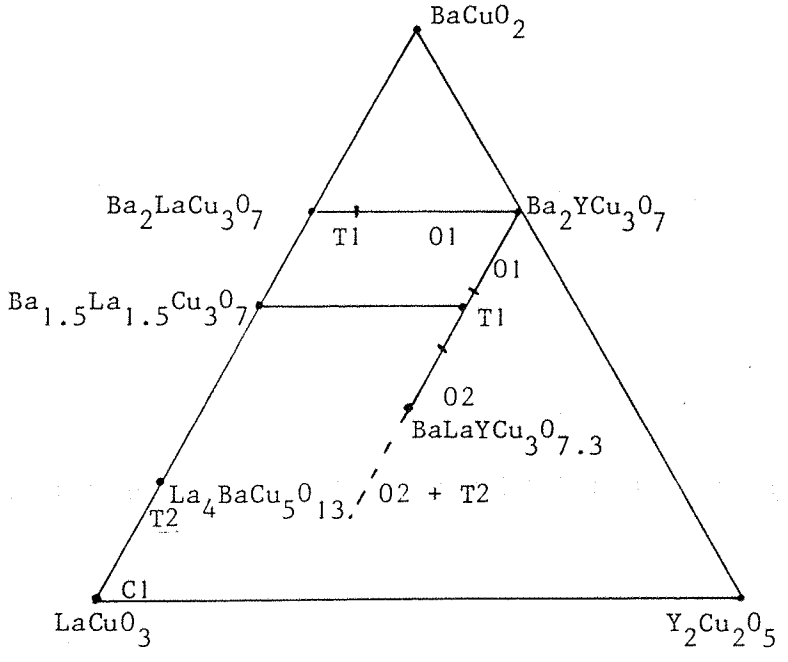

Figure 2.4. Partial Phase Equilibria Diagram for ABO_{3-x} perovskites in the(Ba, La, Y)CuO_{3-x} Chemical System. (R J Cava, 1987c).

3. EXPERIMENTAL TECHNIQUES

In this chapter, the experimental methods for investigating the behaviour of the copper oxide superconductors are briefly described. Experiments were performed to determine the electrical resistivity, a.c.susceptibility and the thermal expansion of the samples.

a. Electrical resistivity.

In as much as zero resistance is an essential characteristic of a superconductor it is natural to make measurements of the electrical resistivity. In any conductor, a study of the variation of resistivity with temperature is useful in determining the nature of possible phase transitions. In a superconductor, the critical superconducting transition temperature T_c is determined. The behaviour of resistivity near the transition temperature T_c can be related to the granularity of the sample (Bednorz and Müller, 1986a). If the material is not superconducting, any evidence of irregular behaviour that may not be apparent in the X-ray diffraction data may be apparent in the electrical resistivity measurement.

The present work deals with the study of the variation of d.c. electrical resistivity of $La_{2+x}Ba_{4-x}Cu_6O_{14+y}$ and related compounds in the temperature range 6K to 300K.

The experimental set up used for the d.c. electrical resistivity measurement was built by Dr P.C. Lanchester. The measurements were done by the conventional four probe method. In this set up, a continuous flow cryostat (Oxford Instruments CF 1200) is used for low temperature measurements. The main vacuum space of the cryostat is maintained at high vacuum $\approx 10^{-6}$ Torr by making use of the pumping system. The pumping system consists of a rotary pump and a diffusion pump. The sample space, provided with a metal plug and an O-ring, is kept vacuum tight. It is evacuated to ≈ 0.1 Torr of Hg using a rotary pump. It is flushed two or three times with

helium and is finally filled with helium (exchange gas). There is an annular space in between the main vacuum space and the sample space. It has a heat exchanger and a thermocouple with its reference junction maintained at 77K in an external liquid nitrogen bath. Liquid helium from a transport dewar is introduced into the annular space through a flexible syphon. This in turn lowers the temperature of the sample due to the presence of the exchange gas in the sample space. The vaporized helium is pumped out of the annular space using a flow pump and is sent through the helium recovery line. This procedure helps in achieving a continuous flow of the liquid in the heat exchanger space. The temperature of the heat exchanger can be controlled by varying the rate of pumping helium. This is done by adjusting a needle valve in the pumping line. A heater is inserted close to the exchanger and can be used if required.

The temperature of the sample was measured by a calibrated silicon diode sensor (Rao and Scurlock, 1983). The silicon diode was fixed very close to the sample. A constant current source was used to send a current of 10 μA through the diode. The diode voltage was fed through an A to D converter the output of which was digitally linearised and then transferred to a BBC computer via the USER port. The resolution obtained in the measurements was $\approx$ 0.1K. The absolute accuracy in temperature measured was $\sim$ 0.5 - 1K.

Another constant current source was used to send a current of 1-10 mA through the sample. The value of the current sent through the sample was decided depending on the heat dissipation factors. The current density through the sample was maintained at 0.1 -0.2A/cm^2. A digital voltmeter (Solartron) having a resolution of 100 nV was used to record the voltages across the leads to the sample. The DVM was interfaced to the computer via an IEEE port. The block diagram of the data acquisition system is shown in Fig.3.1.

The sintered sample was cut to a rectangular shape (8mm x 5mm x 1mm). The dimensions of the sample, viz the width and the thickness were measured with a micrometer. The current and the voltage

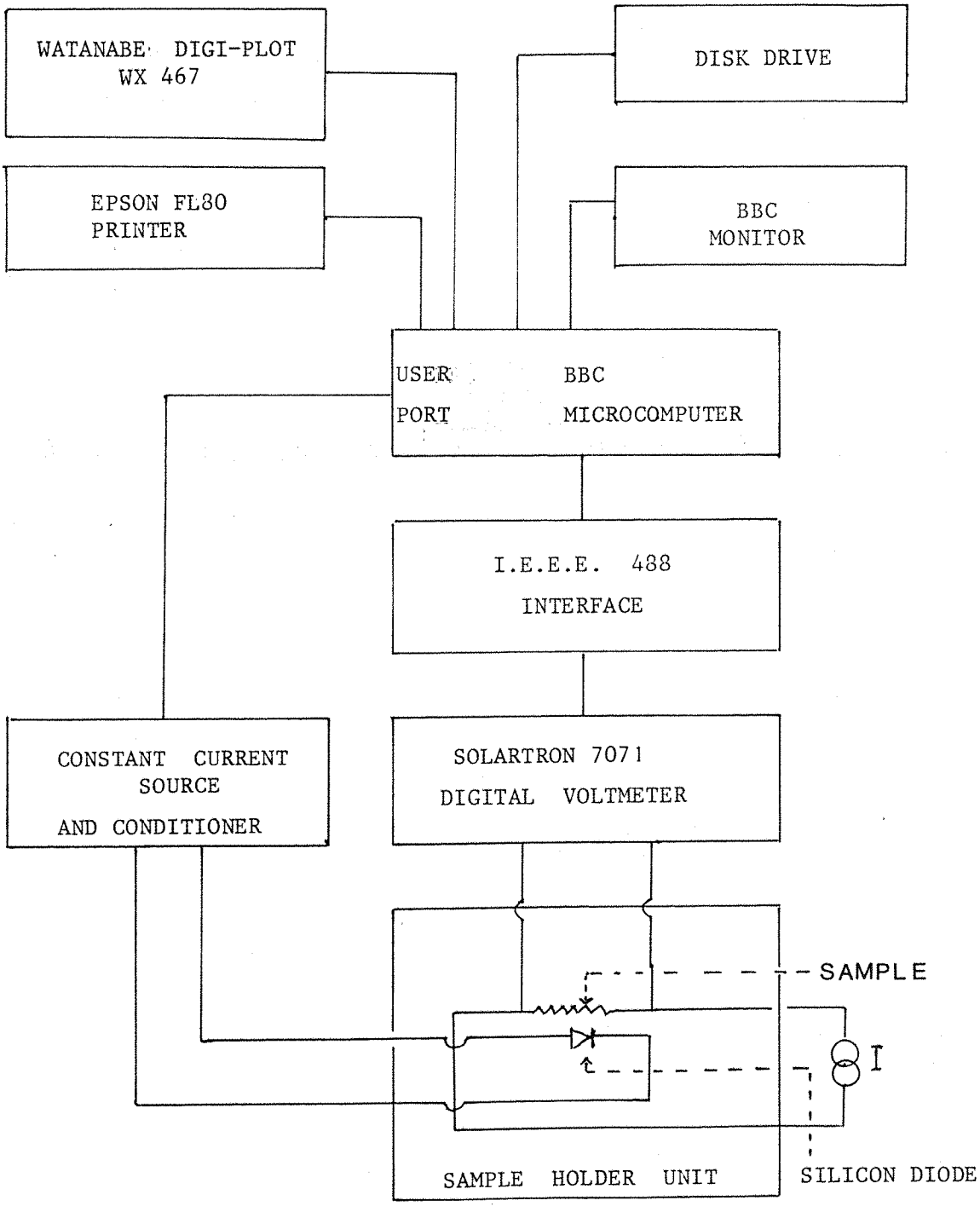

Figure 3.1. Data Acquisition System for Resistivity Measurement.

leads were attached to one of the faces of the sample by silver paint. Care was taken to see that the contact resistance was as small as possible ($\approx 1\Omega$). If the contact resistance was high, it would give rise to Joule heating. The distance between the voltage leads was measured with a mm scale. Uncertainty in this measurement was the main source of error in the absolute measurement. When the silver paint dried up, the sample was mounted on a tufnol sample holder which was fixed to a long stainless steel tube. The leads from the sample and the silicon diode were anchored to the pin provided on the other end of the stainless steel tube. The sample holder assembly was then inserted into the cryostat.

The transfer syphon was flushed with helium. One arm of the syphon was inserted into the syphon inlet of the cryostat. The other arm of the syphon was slowly let into the helium transfer vessel. The continuous flow pump and the temperature controller were switched on and the flow valve was adjusted so as to obtain a rate of decrease of temperature $\approx$ 2K/minute. Thermal emfs were negligible with a slow cooling rate. Failure to cool sometimes occurred due to the blockage inside the syphon, and the blockage had to be cleared by taking the syphon out and flushing it with warm helium gas.

A computer program in BASIC, written by Dr P.C. Lanchester, was used to monitor the time, the temperature of the sample, the voltage across the leads and the thermal emf that was present due to the temperature gradient. The computer measured the thermal emf by periodically turning the sample current off. The sample was cooled from room temperature to $\approx$ 6K.

The sample was allowed to warm up gradually by adjusting the flow valve. This was done until the temperature of the sample reached about 40 or 50K. Afterwards, the flow pump was put off and the sample was warmed up gradually by manually controlling the heater.

The data was analysed by making corrections for the thermal emf at each temperature. The data of resistivity vs temperature was stored on the floppy disc and plotted using the plotter.

b. a.c. susceptibility.

The a.c. susceptibility measurements serve as an important tool to investigate the flux exclusion associated with superconductivity. The diamagnetic shift below the critical transition temperature arises from the shielding effect of the normal and the superconducting components of the material. The measurements are useful in determining the upper limit of the superconducting volume fraction of the material corresponding to the perfect flux exclusion (diamagnetism).

The a.c.susceptibility measurements have been done using an existing apparatus which was recently improved by Dr R.J. Pulham. There are two primary coils connected in series and the concentric secondary coils are each wound in opposite direction. The sample is placed inside one of the secondary coils. An oscillatory current is sent through the primary coil. The induced emf across the secondary coil is proportional to the magnetization of the sample and hence it depends on the susceptibility of the sample.

An alternating magnetic field is set up around the sample by exciting the primary coil with a constant a.c. current. The frequency of the applied field is kept constant at 325 Hz. The circuit that is employed for measuring the susceptibility is shown in figures 3.2 and 3.3. The measuring field can be taken as that present at the centre of the specimen. Figure 3.2 shows the block diagram of the driving system and the impedence matching circuits. Figure 3.3 shows the sine wave generator and the feed back circuitry, which ensures that the magnitude of the exciting current through the primary coil is kept constant. Hence any change in the signal induced in the secondary coils will be due to a change in the permeability of the medium between the primary and the secondary coils. When the

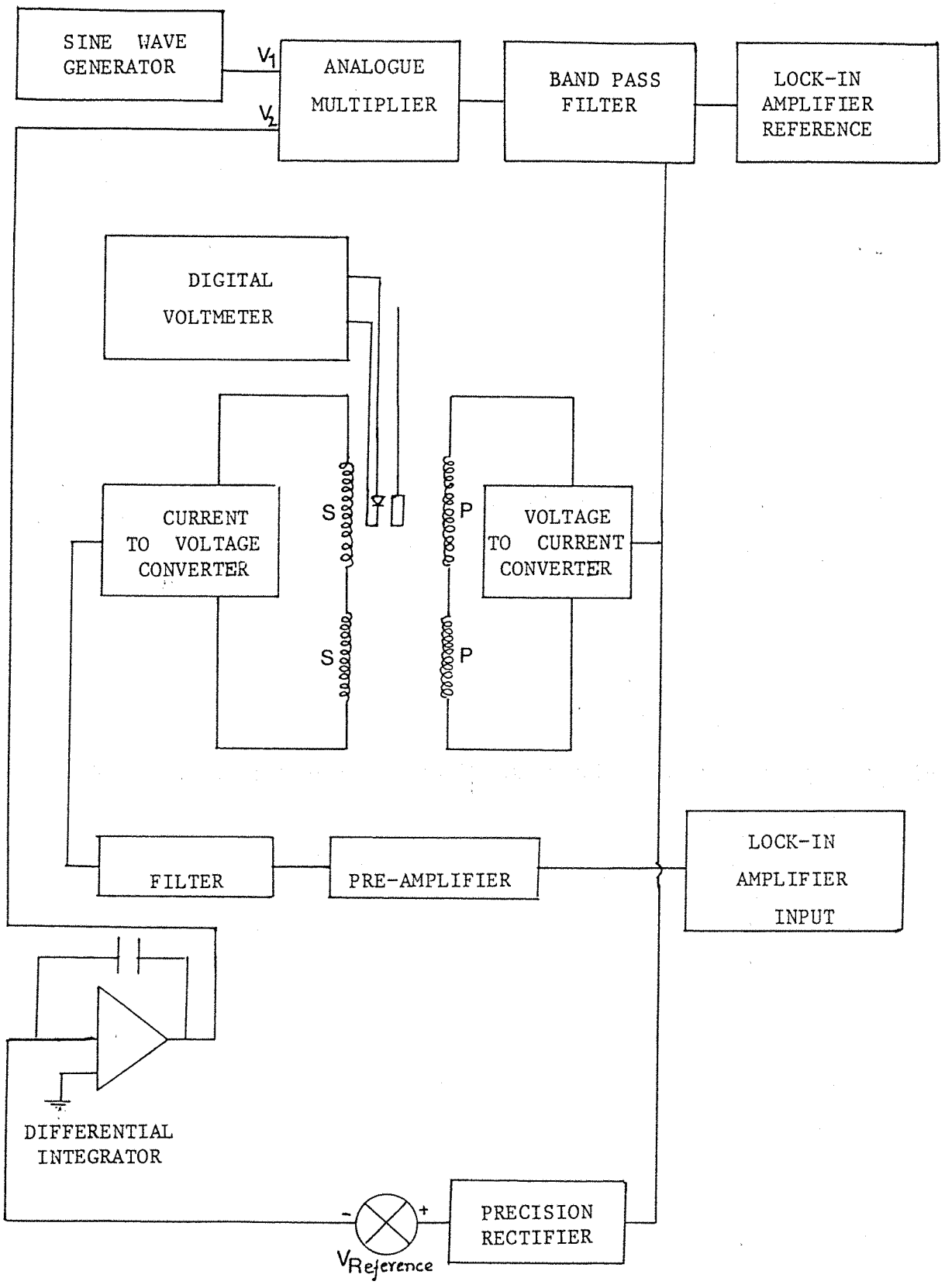

Figure 3.2. Block Diagram of the a.c. Susceptibility Apparatus.

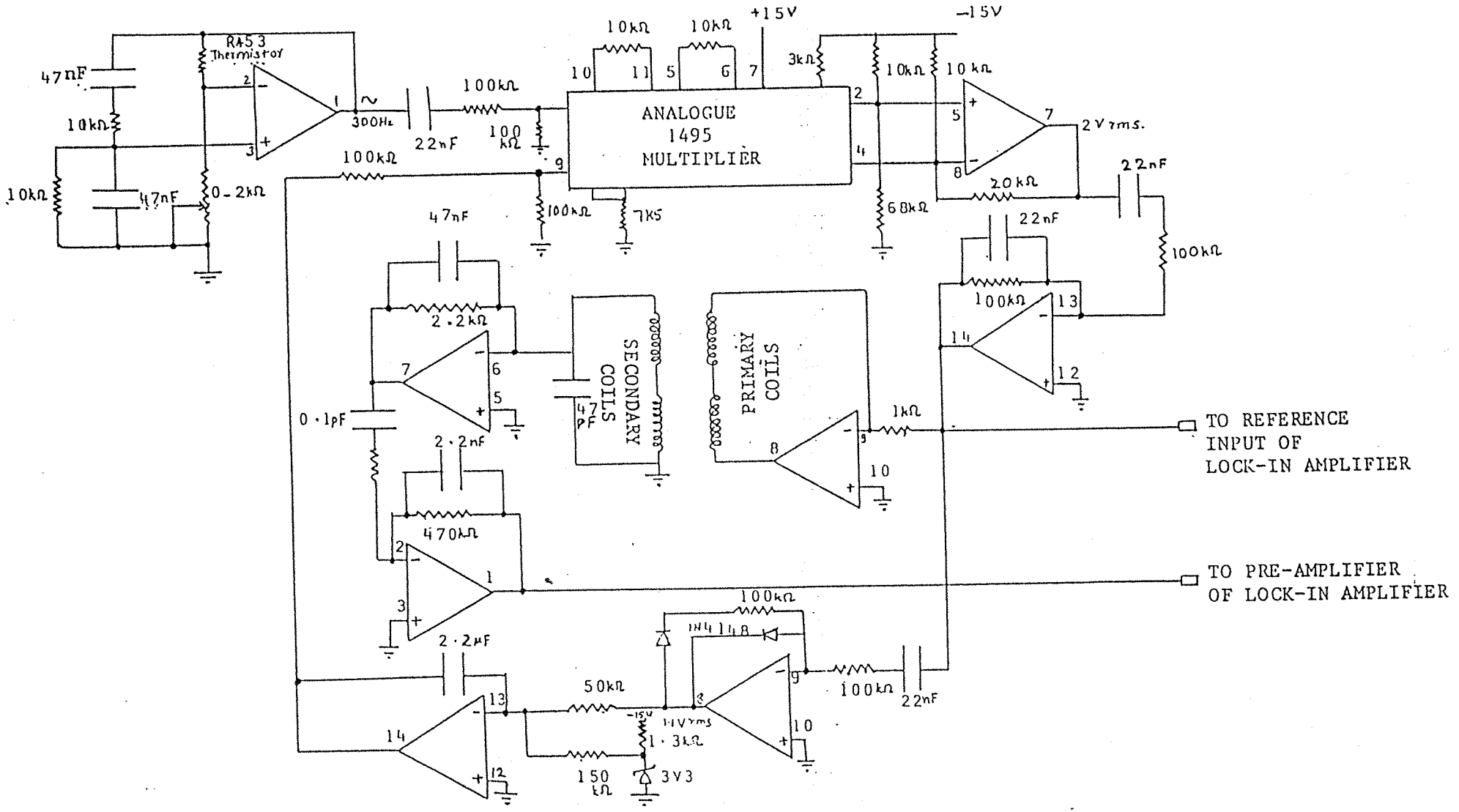

Figure 3.3. a.c.Susceptibility Drive and Conditioning Circuitry.

specimen is introduced, the change in the mutual inductance of the coils is given by

$$\Delta M = n_s n_p V \chi A$$

where n_s and n_p are the number of turns/unit length of the primary and secondary coils. V is the volume of the specimen and χ is its susceptibility. A is a factor depending on the geometry of the coils.

When a current I at a frequency ω passes through the primary coil, the difference in the voltages across the secondary coil with and without the sample placed in it is given by

$$\Delta V = I\omega \Delta M$$

The a.c. magnetic susceptibility is a complex quantity and is given by

$$\chi = \chi' - i\chi''$$

where χ' is the in phase component to the magnetic field and χ'' is the out of phase component due to the hysteresis effects and eddy currents and is proportional to the energy dissipation.

The signal voltage v_i induced in the secondary coil inevitably carries noise due to the resistive and electrostatic coupling across the coils. A lock-in amplifier (LIA) is used to measure the inductively coupled signals v_i. The LIA uses a reference signal at the same frequency as the input signal v_i. In fact, both the reference and the signal frequencies are derived from the same source and the detector effectively 'locks in' to the signal frequency v_i.

The signal to noise ratio is enhanced by passing the signal through a low pass filter. The high frequency components are removed. Only the Fourier components of the noise voltage with

frequencies near the signal frequency will contribute to v_o. The bandwidth $\Delta\omega$ of the detector is given by the inverse of the time constant. The time constant used in the circuit is 3 seconds.

The phase of the reference signal v_r is adjusted with respect to the input signal v_i so that the magnitude of the detected signal component is maximized.

The above processing results in the output v_o consisting of a d.c. term which is proportional to the amplitude of the signal v_i.

The sintered sample weighing about 0.39 gm was mounted on a tufnol sample holder which was fixed to a non-magnetic stainless steel tube. A silicon diode fixed in close thermal contact with the sample was used as a temperature sensor. A constant current source was used to send a current of 10 μA through the silicon diode. A digital voltmeter was used to monitor the forward bias voltage. The voltage measured was a unique function of temperature. The sample holder along with the assembly of the mutual inductance coils was inserted into the cryostat as in the resistivity rig.

Before each measurement, the temperature of the sample was stabilized. This was necessary to minimize the thermal gradients over the coil set which causes instabilities in the detected voltage. Temperature stability was maintained by adjusting the helium flow valve so that the temperature of the cryostat as measured by the thermocouple fell 2 or 3K below the required temperature which was the 'set point' on the temperature controller (Oxford Instruments). The automatic heating stabilized the temperature to the set value. The difference in the output signal v_o when the sample is in and the sample is out of the secondary coil is obtained at different steady temperatures

$$V_0 = \text{constant} \times \chi' \ .$$

The constant of proportionality was determined by a calibration where

we used high purity lead. For lead we know that $T_c \leq 7K$ in low magnetic fields and its volume susceptibility is equal to -1 (perfect diamagnetism).

The advantage of this method is that the a.c. susceptibility measurements give directly the T_c without need of making contact to the sample.

c. Thermal expansion.

The study of thermal expansion provides information regarding the vibrations of the crystal lattice (Barron et al 1980). The coefficient of thermal expansion of a material is given by

$$\alpha = \frac{1}{\ell} \frac{\partial \ell}{\partial T}$$

where $\partial \ell$ is the change in length, ℓ is the original length of the specimen and ∂T is the increase in temperature. Thermal expansion occurs due to the anharmonic nature of the interatomic forces in a solid. It is a structure sensitive property and exhibits an anomaly whenever a material undergoes a structural phase transition. Other phase transitions such as magnetic, electronic and superconducting transitions often contribute to the total thermal expansion coefficient.

The behaviour of the thermal expansion of $YBa_2Cu_3O_7$ has been investigated. The thermal expansion of the sintered polycrystalline sample was measured using a three terminal capacitance method. The method employed is one of the most sensitive methods and was developed by G.K.White. This technique determines the change in the capacitance induced by a change in the length of the sample as the temperature is varied. The method compares the dilatometer capacitance with a standard capacitor using an a.c. bridge (Thompson A.M., 1958). The block diagram of the thermal expansion data acquisition system is as shown in figure 3.4 (R.J.Pulham, 1987).

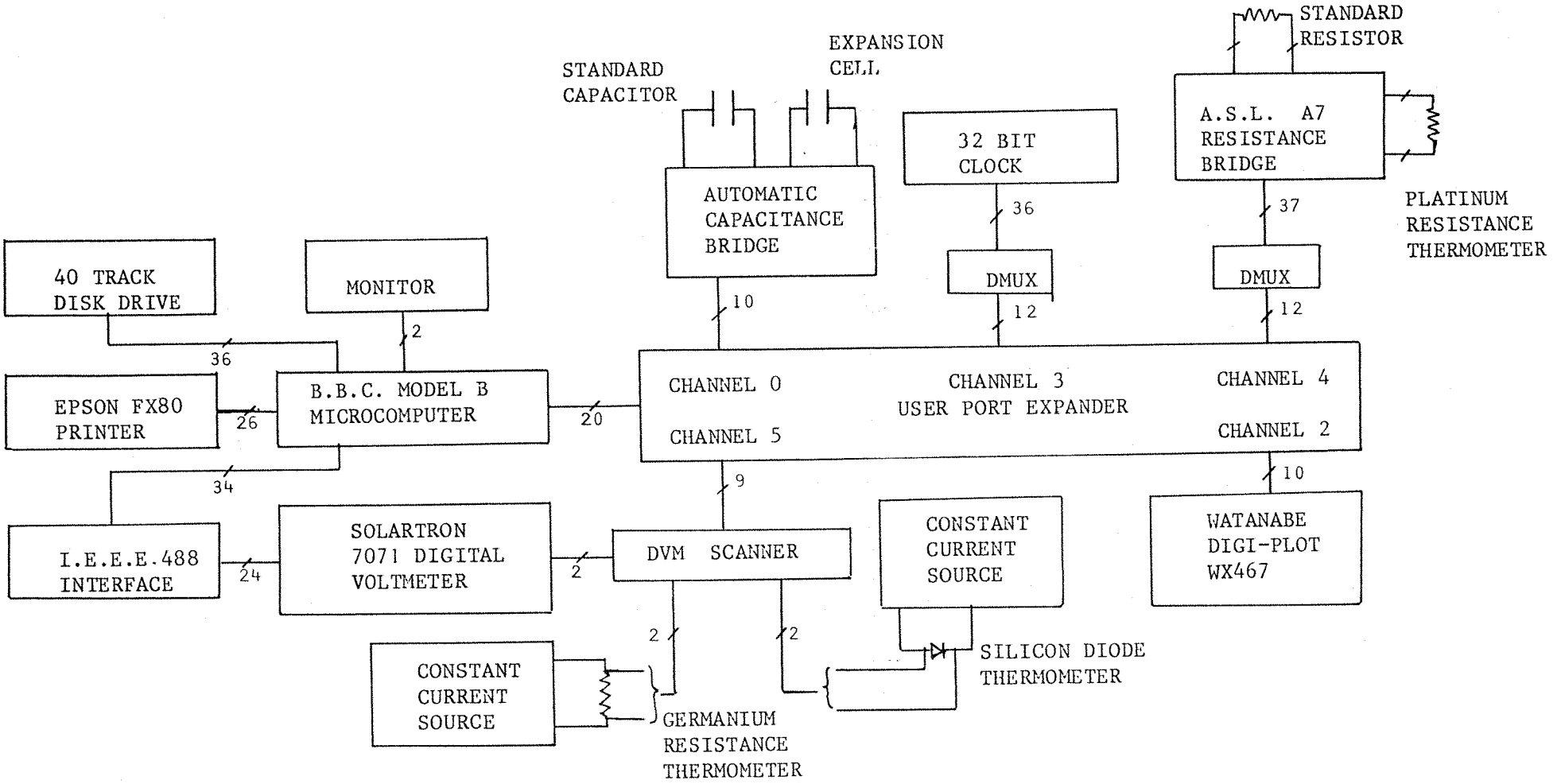

Figure 3.4. Data Acquisition System of thermal expansion (R J Fulham, 1987)

The automatic self balancing capacitance bridge was designed and built by Dr.R.J.Pulham (1987). The basic principle that is involved can be described with reference to figure 3.5. The carrier generator excites a step up transformer which provides signals of equal and opposite phase to both arms of the bridge. The signal applied to C_s is reduced by an inductive voltage divider, whereas the dilatometer with the unknown capacitance C_x carries the full bridge voltage. Both C_s and C_x are three terminal capacitors. For null balance of the detector, the two currents from both arms of the bridge must be equal and opposite. This gives the balance condition of the bridge:

$$nC_s = C_x .$$

Thus the ratio of C_x to C_s is proportional to the ratio of the inductive voltage divider. The ratio of the inductive voltage divider is controlled via the software of the automatic capacitance bridge (A.C.B) and the ratio is transferred to the BBC through an interface. The operation of the A.C.B. is explained in great detail by R.J.Pulham (1987).

The expansivity measurements were done using the expansion cell which has been used for determining the expansivity of iron difluoride and magnetic rare earth intermetallic polycrystalline compounds. The data for $YBa_2Cu_3O_7$ was inconclusive. It suggested that the data was influenced by two factors. One factor could be due to G.E. varnish used to place the sample in between the cell base and the capacitor plate. The other factor could be due to the expansion of the cell material. The expansion of the cell material (Cu) is much greater than that of the copper oxide ceramic.

To avoid spurious results due to the G.E. varnish the expansion cell was modified. The thermal expansion of $YBa_2Cu_3O_7$ was measured with this modified cell.

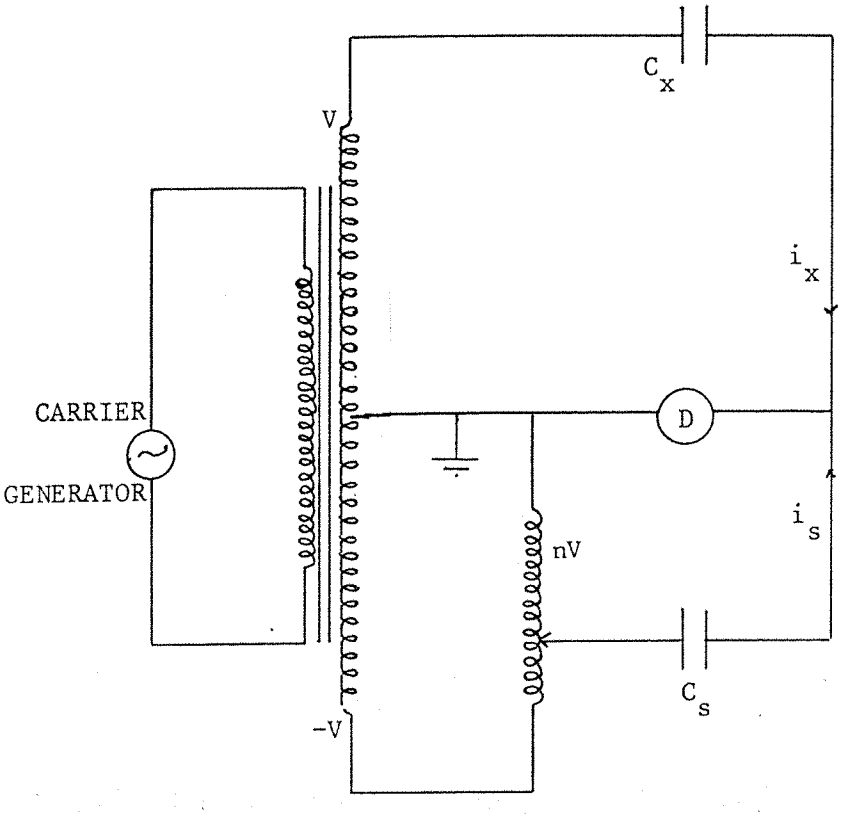

Figure 3.5. Basic A.C Bridge

A schematic cross section of the expansion cell is shown in figure 3.6. The OFHC copper has been used for the cell material. The cell consists of the base plate, the high potential capacitor plate H and the low potential plate L. The low potential plate is separated from the guard ring by epoxy resin. The base plate is held in position by means of the threaded supports and the adjustment collars. The sample is placed between the cell base and the high potential capacitor plate by using the three screws and the associated springs. The guard ring is anchored to the top plate of the sample holder. It produces a uniform electric field between the capacitor plates and eliminates the edge effects. A platinum resistance thermometer is thermally anchored to the base close to the sample. The expansion cell is connected via a tufnol mount (not shown in the diagram) to the cryostat sample holder. The leads from the expansion cell are taken through the tufnol mount and are thermally anchored to the top of the sample holder rod. The expansion cell is enclosed in a copper can and the space inside is made vacuum tight by indium seal.

The cryostat consists of a liquid nitrogen shield and the liquid helium bath (main bath). The space surrounding the main bath and the liquid nitrogen jacket is maintained at high vacuum by making use of a rotary and a diffusion pump. A variable temperature insert is located in the main bath and draws the liquid coolant from the bath through a syphon into a heat exchanger. The liquid coolant is vaporized and leaves through an annular exhaust surrounding the sample holder space. The cooling power is transferred to the sample holder via the helium exchange gas. Accurate adjustment of the flow of gas through the exhaust is effected via a continuous flow pump and the flow valve. The sample holder space and the variable temperature insert are otherwise thermally isolated from the main bath by the inner vacuum space and the radiation shields.

The temperature of the sample is measured by a platinum resistance thermometer. The resistance of platinum is measured by an automatic A7 resistance bridge (ASL Labs). The ratio of the

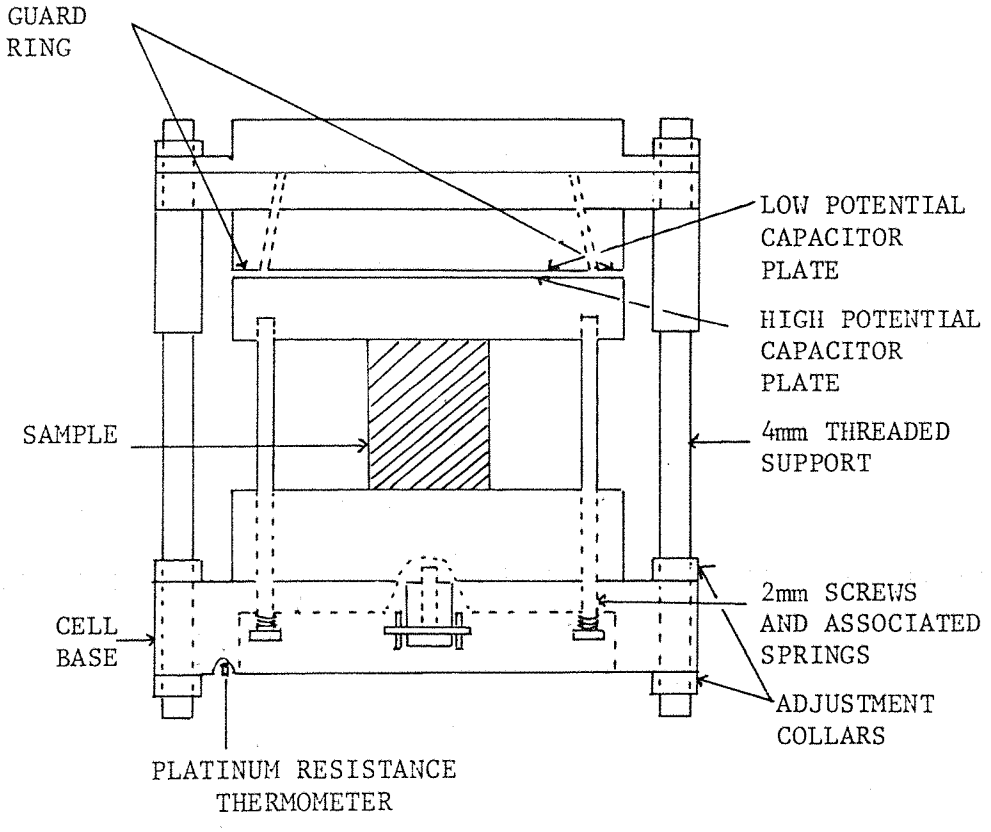

Figure 3.6 Expansion Cell.

resistances of the sensor and a standard resistor is recorded at each temperature and the data is transferred to the computer. The resolution of the A7 bridge is 0.1 mK at the temperature of these measurements and is accurate to about 2 mK.

A silicon diode is mounted on the stainless steel tube carrying the copper can. It is used for measuring the temperature of the sample holder space. The silicon diode forward voltage drop is measured by the DVM interfaced to the microcomputer.

The length of the sample is measured with a micrometer gauge. Its two mounting surfaces should be perfectly flat. The high tension plate is held carefully and the collars are adjusted so that the sample can be placed on the base and the distance between the capacitor plates is about a fraction of a mm. The three screws provided to hold the high potential capacitor plate are adjusted so that the plate rests squarely on the sample. The capacitance between the plates is measured by a (manual) bridge with an accuracy of 2pF over a range 0-100pF. The capacitor gap is now adjusted using the adjustable collars of the three threaded support rods to move the base plate up or down. The capacitance is adjusted to be between 20-30 pF. The brass can is now replaced with the indium seal and the whole sample holder assembly is carefully inserted into the sample holder space of the cryostat.

The automatic capacitance bridge is now calibrated using a 10 pF standard capacitor. This is done by manually adjusting the decade switches in sequence to get a null balance at a high gain setting and then calibrated automatically. Then the bridge is switched to operate on the serial automatic balance mode and the balance is again checked. The 10 pF capacitor is disconnected and in its place, the leads from the dilatometer cell are connected. The bridge is now switched on to the manual mode and only the first two decade values are adjusted to get a rough balancing on the detecting meter. The bridge is then switched on to the serial mode and the balance checked.

The computer programs (R.Pulham, 1987) are used to test all the different units used in the experimental set up and the automatic recording of the dilation. The testing program is loaded on the computer.

The sample space and the sample holder space are evacuated to a pressure of 10^{-2} Torr and filled with helium. The main vacuum and the inner vacuum space should be maintained at a pressure of 10^{-5} Torr or less.

The main bath is filled with liquid nitrogen using the transfer syphon inserted in the entry port. When the bath is completely filled with nitrogen the transfer syphon is removed and the valve on the main bath closed. The outlet from the main bath is provided with a bunsen valve through which the nitrogen gas from the main bath can escape to the atmosphere. The flow pump is switched on and the flow valve opened. From now onwards the temperature of the sample space and the sample holder space are continuously monitored. The flow valve is adjusted so that the sample cools gradually. In the beginning the temperature of the sample holder space is less than the sample temperature by a few K. When the sample is reaching equilibrium with its surroundings, the difference between the temperatures of the sample space and the sample holder space is of the order of 10mK. The flow pump is switched off and the system is left to warm up by a few degrees for about four hours. Then the bath is pumped out and flushed with helium gas.

Liquid nitrogen is filled in the shield and liquid helium is transferred to the main bath through the entry port. During the cooling procedure, care is taken to see that the needle valve is not blocked. The flow pump is switched on and the main bath is filled to about three-fourths of its volume as indicated by the helium level indicator.

The control program effects a continuous recording of temperature of the sample, the ratio of the standard and dilatometer capacitances and the time as reckoned by the 32-bit clock. After every 50 readings, the average temperature, the average ratio, the standard deviation for temperature and ratio and the rate of change of capacitance with time $\frac{dC}{dt}$ are computed by fitting the data of ratio vs time to a straight line using a least square routine. The same fit is worked out for $\frac{dT}{dt}$ and rejecting readings outside the standard deviations and then refit until no readings are rejected. $\frac{dC}{dT}$ is finally computed.

During the experiment the temperature of the sample was found to change very slowly at 77K. The resolution of the A7 bridge was changed from 10^{-5} to 10^{-6}. The pre-amplifier gain was changed from 1 to 100. The flow pump was put off when the sample temperature was about 130K. The data was recorded until the sample warmed up gradually to 240K.

The expansivity of the sample was calculated as follows:
For an ideal parallel plate capacitor, the capacitance

$$C_o = \varepsilon \frac{\pi r^2}{d} \qquad (3.1)$$

where r is the radius of the low potential capacitor plate, d is the distance between the plates. ε is the permittivity of free space.

The corrections are made for the non-parallelism of the capacitor plates (Tilford 1969) and the distortion of the electric field near the edge of the capacitor plates (White, 1961). Hence, the effective value of capacity is given by:

$$C = \frac{\varepsilon \pi r^2}{d} \left[1 + \frac{1}{16} \left(\frac{\Delta d}{d} \right)^2 + \frac{xd}{r(d+0.22x)} \right] \qquad (3.2)$$

where Δd is the capacitance gap change that occurs due to the tilting of the capacitor plates. x is the width of the gap between the guard ring and the capacitor plate.

In the method, we used for setting the capacitance gap (Legg, 1980), $\frac{\Delta d}{d} = 0.2$.

The rate of change of capacitance with respect to temperature is given by (Legg, 1980; R.J. Pulham, 1987)

$$\frac{dC}{dT} = \frac{\partial C}{\partial d} * \frac{\partial d}{\partial T} + \frac{\partial C}{\partial r} * \frac{\partial r}{\partial T} \qquad (3.3)$$

$$\frac{\partial C}{\partial d} = - A_1 \frac{C_o}{d}$$

where $A_1 = \left[1 + \frac{3}{16} \left(\frac{\Delta d}{d} \right)^2 + \frac{xd^2}{r(d+0.22x)^2} \right]$

$$\frac{\partial C}{\partial r} = \frac{2A_2 C_0}{r}$$

where $A_2 = \left[1 + \frac{1}{16} \left(\frac{\Delta d}{d} \right)^2 + \frac{xd}{2r(d+0.22x)} \right]$

$$\frac{\partial r}{\partial T} = \alpha_{Cu} r$$

where α_{Cu} = thermal expansion of copper.

$$\frac{\partial d}{\partial T} = - \left(\alpha_{Cu} - \alpha_{sample}\right) L = \alpha^1 L$$

where L is the length of the sample. Change in the capacitance gap is related to the expansion of the cell material (Cu) and the sample.

Substituting for the above expressions in equation (3.3),

$$\frac{dC}{dT} = - A_1 \frac{\alpha^1 L C_0}{d} + 2A_2 C_0 \alpha_{Cu}$$

Substitution for α_{Cu} is made from the data of Kroeger and Swenson (1977).

Expansivity of the sample is determined from the equation

$$\alpha_{sample} = \alpha_{Cu} \left(1 - \frac{A_2}{A_1} \frac{2d}{C_0} \right) + \frac{d}{L A_1} \frac{1}{C_0} \frac{dC}{dT}$$

The data of α_{sample} at each temperature is obtained by using another computer program.

The normalized length change, $\frac{\Delta \ell}{\ell}$ is computed at each temperature by making use of the expansivity data (R.Pulham, 1987).

$$\frac{\Delta \ell}{\ell} = \sum_{n=1}^{m} \alpha_n T_n$$

where α_n and T_n denote the thermal expansivity and the average temperature of the n^{th} data set.

4. RESULTS

The $YBa_2Cu_3O_7$ and $La_{2+x}Ba_{4-x}Cu_6O_{14\pm y}$ compounds used in our measurements were prepared by Dr Mark T. Weller and Mr J R Grasmeder in the Chemistry Department. The results of thermal expansion, resistivity and a.c. susceptibility measurements will be reported in this chapter.

a. Resistivity of $La_{2+x}Ba_{4-x}Cu_6O_{14\pm y}$ and related compounds

The resistivity behaviour of the following compounds were investigated:

1. $La_{2+x}Ba_{4-x}Cu_6O_{14\pm y}$ (x=0,0.2,0.4,0.6,0.8)

2. $La_{1.5}(Ln)_{1.5}Ba_3Cu_6O_{14\pm y}$ (Ln = Y, Yb)

3. $Y_2La_xBa_{4-x}Cu_6O_{14\pm y}$ (x = 0.2, 0.6)

All the samples belong to the group ($A_6Cu_6O_{14\pm y}$) where A is a mixture of divalent and trivalent ions. Oxides like $YBa_{2-x}Sr_xCu_3O_{7-y}$ and $Yb_xEr_{1-x}Ba_2Cu_3O_{6+y}$ are typical examples.

The polcrystalline samples were prepared by the direct oxide technique. High purity 99.99% metal oxides La_2O_3,CuO,BaO,Y_2O_3 were used for sample preparation. The dry oxides were taken in the appropriate ratio and were ground thoroughly. The mixture was heated at 900°C for 24 hours in air. It was reground and heated at 950°C for 48 hours in pure oxygen. Unannealed samples were obtained by rapid quenching of the samples.

The annealed samples were slowly cooled to room temperature. The pellets were compacted at a pressure of 7.5 x 10^8Pa and reannealed in oxygen at 450^{o}C. All the samples prepared were of single phase. The oxygen stoichiometries of all the samples have been determined by thermogravimetric analysis.

All the compounds belonging to the above groups have their structures lying between the orthorhombic $Y_2Ba_4Cu_6O_{14}$ and the tetragonal symmetry of $La_3Ba_3Cu_6O_{14}$ (M T Weller, 1987). The annealing temperature and the oxygen pressure seem to be the deciding factors in controlling the structure.

1.a. $La_{2+x}Ba_{4-x}Cu_6O_{14}$ (unannealed compounds)

The above group of compounds were studied for compositions with x=0.0,0.4,0.6 and 0.8. Their resistivities increase as the temperature is lowered from room temperature i.e. a purely semiconducting behaviour is seen. On further lowering the temperature (below 75K for x=0) the resistivity decreases and at still lower temperatures an upturn in the behaviour is observed (figure 4.1).

1.b. $La_{2+x}Ba_{4-x}Cu_6O_{14+y}$ (annealed compounds)

The resistivities of these compounds are much lower than those of unannealed samples (Table I). All the samples exhibit a superconducting behaviour. When x=0, the resistivity decreases rather slowly until the onset of superconductivity is reached. When x=0.6, the resistivity shows a metallic behaviour down to 80K and then develops a shoulder before the onset of superconductivity (Figure 4.3). The sample with x=0.8 shows a resistivity drop at 50K (Figure 4.4). Although it tends to show a transition as in the other four cases, it is not superconducting down to 6K. The resistivity characteristics show that as the La concentration

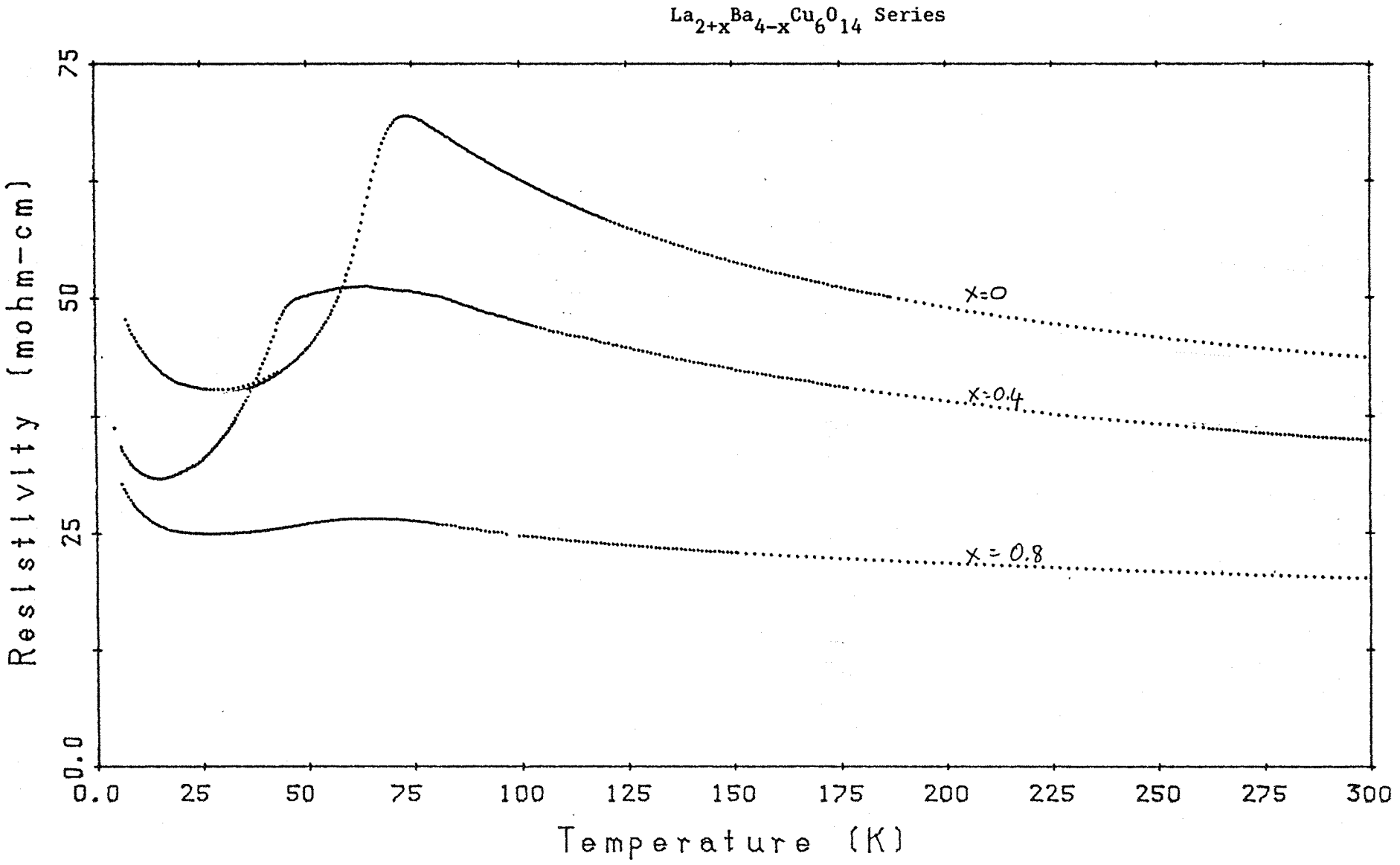
La2+xBa4-xCu6O14 Series
Resistivity (mohm-cm)
75
50
25
0.0
0.0
25
50
75
100
125
150
175
200
225
250
275
300
Temperature (K)
x=0
x=0.4
x=0.8

Figure 4.1.

increases from x=0 to x=0.6, the transition temperature is shifted to lower temperatures. The compound with x=0 has a maximum value of T_c (≈ 65K) (Figure 4.2). T_c refers to the mid-point of the transition.

2. $La_{1.5}(Y/Yb)_{1.5}Ba_3Cu_6O_{14+y}$

The La sites are partially occupied by Y^{3+} in the stoichiometry $La_{1.5}Y_{1.5}Ba_3Cu_6O_{14+y}$. The resistivity at room temperature is very low and the compound shows a semiconducting behaviour. When Yb^{3+} is substituted for La^{3+}, the data shows a semiconducting behaviour and an anomaly at ≈ 85K (Figure 4.5). The resistivity decreases and starts increasing at ≈ 62K.

Table I **Resistivity of $La_{2+x}Ba_{4-x}Cu_6O_{14}$ compounds at room temperature**

x	ρ (m Ω cm)	
	unannealed samples	annealed samples
0	40.93	66.82
0.2	(139.2)	3.0
0.4	35.05	3.1
0.6	20.2	2.645
0.8	20.26	7.95

3. $Y_2La_xBa_{4-x}Cu_6O_{14+y}$

The resistivity characteristics indicate a metallic behaviour until the onset of superconductivity is reached. The samples with x=0.2 and 0.6 are superconducting with T_c equal to 93K and 60K respectively (Figure 4.6). The resistivities of these samples at room temperature are of the same order as that of 1b samples.

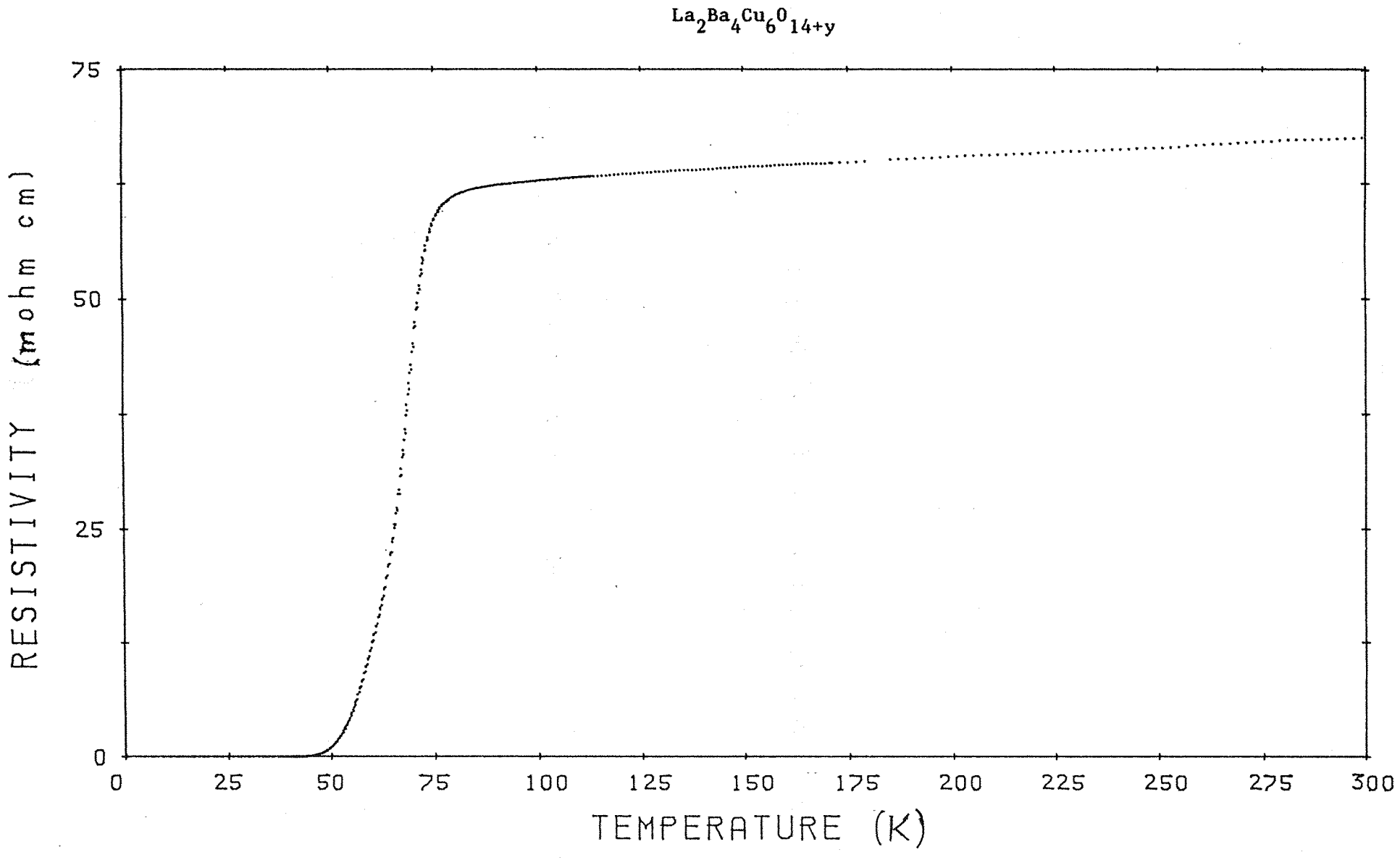
$La_2Ba_4Cu_6O_{14+y}$
RESISTIVITY (mohm cm)
75
50
25
0
0
25
50
75
100
125
150
175
200
225
250
275
300
TEMPERATURE (K)

Figure 4.2.

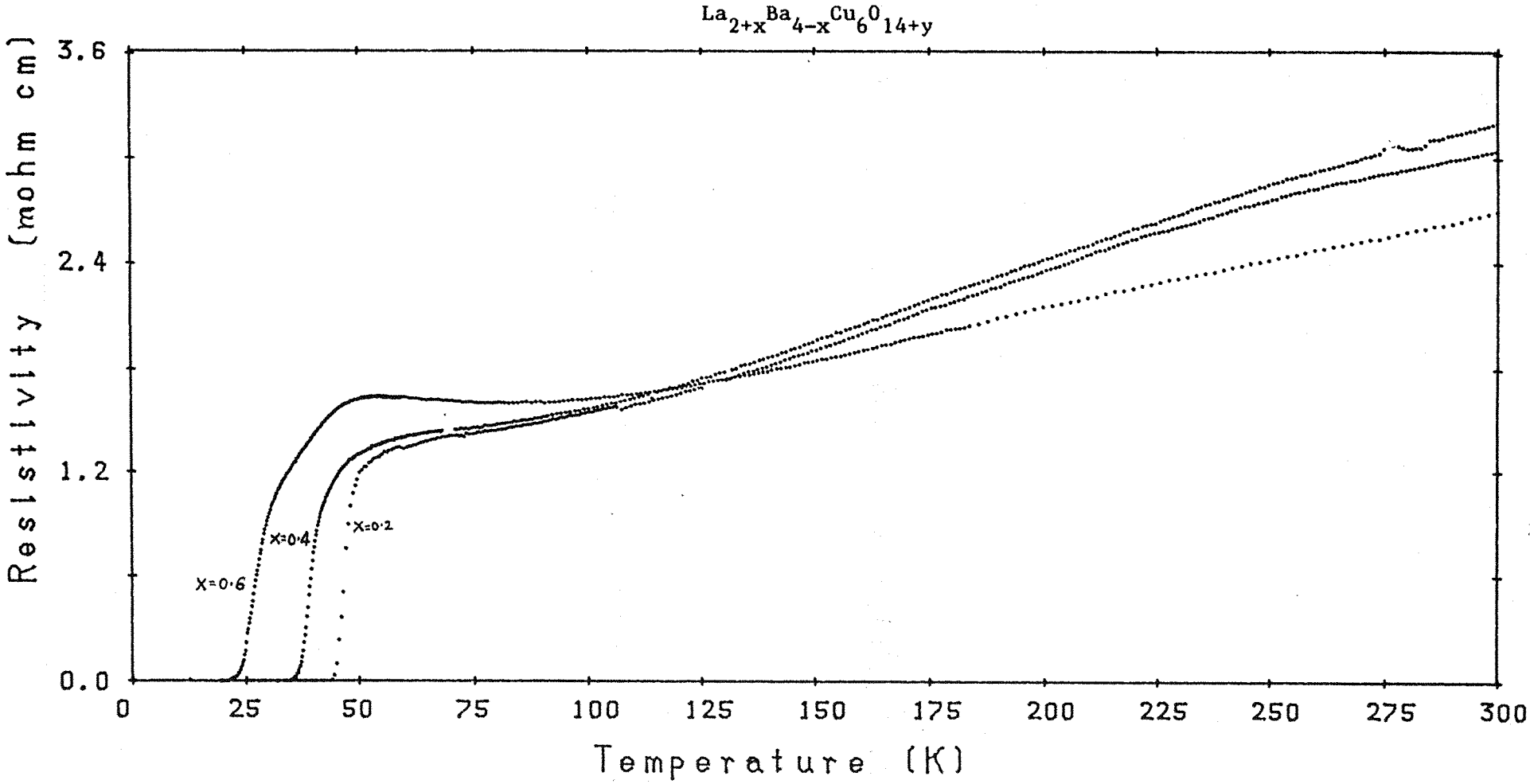
$La_{2+x}Ba_{4-x}Cu_6O_{14+y}$
Resistivity (mohm cm)
3.6
2.4
1.2
0.0
0
25
50
75
100
125
150
175
200
225
250
275
300
Temperature (K)
X=0·6
X=0·4
X=0·2

Figure 4.3.

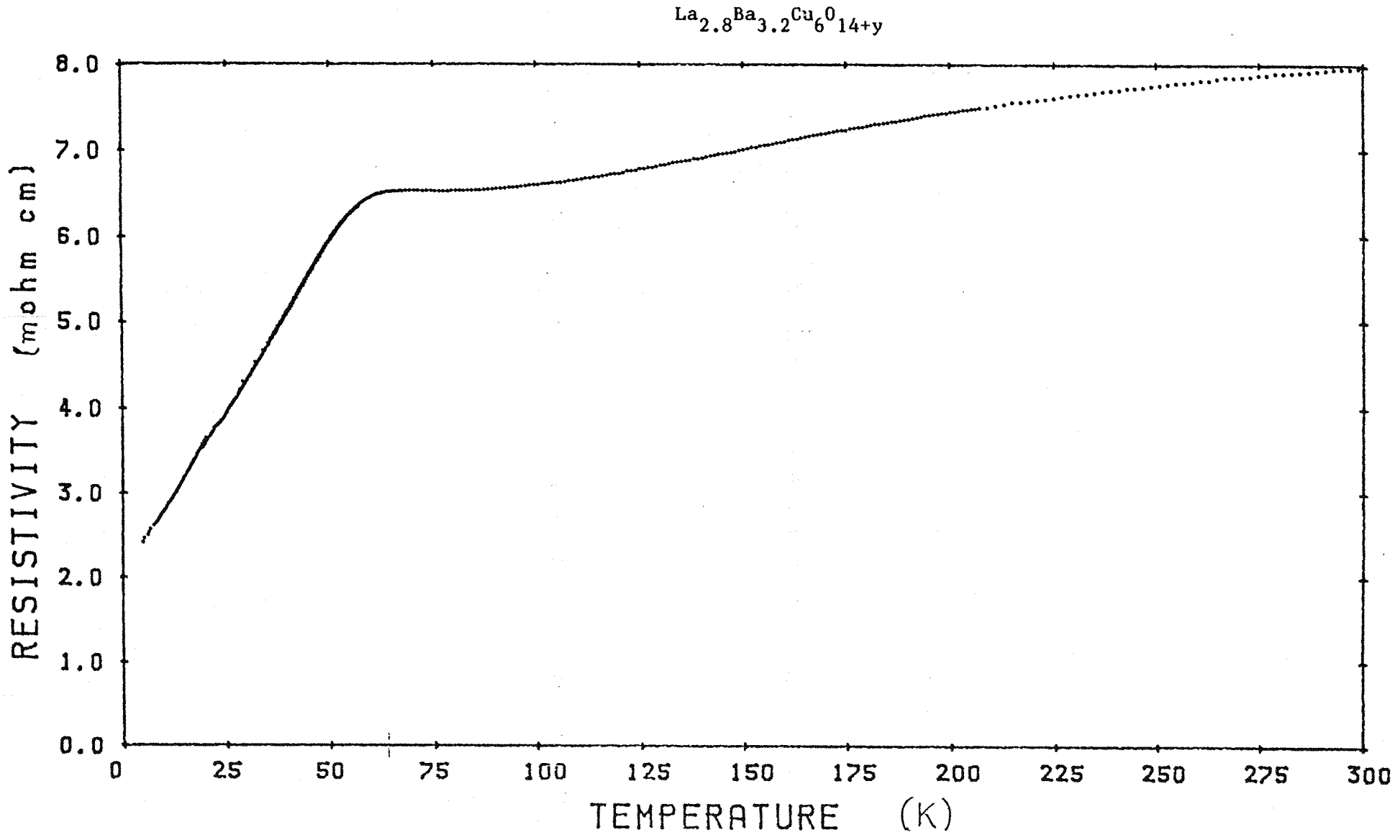
$La_{2.8}Ba_{3.2}Cu_6O_{14+y}$
RESISTIVITY (mohm cm)
8.0
7.0
6.0
5.0
4.0
3.0
2.0
1.0
0.0
0
25
50
75
100
125
150
175
200
225
250
275
300
TEMPERATURE (K)

Figure 4.4.

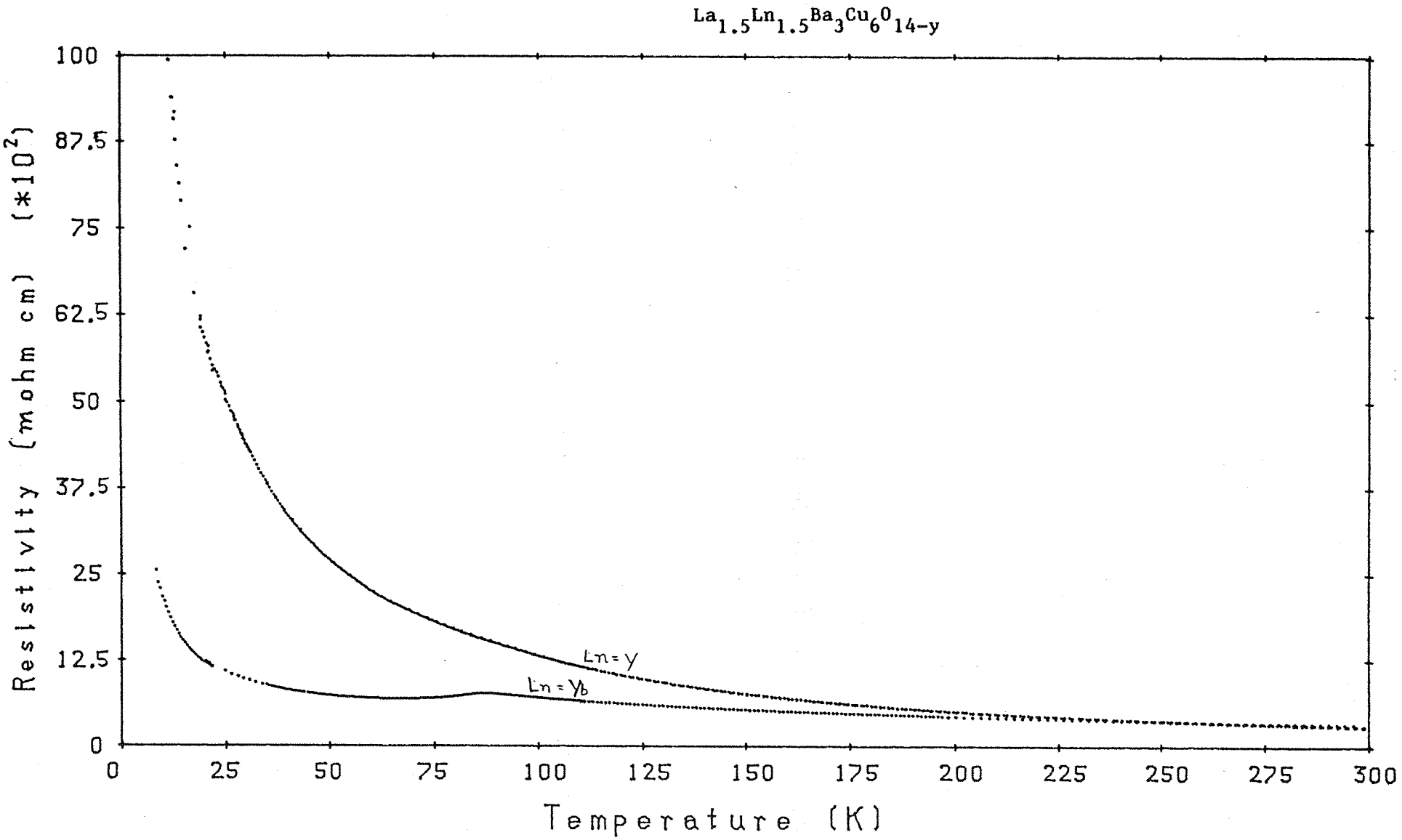
$La_{1.5}Ln_{1.5}Ba_3Cu_6O_{14-y}$
Resistivity (mohm cm) (*10²)
100
87.5
75
62.5
50
37.5
25
12.5
0
0
25
50
75
100
125
150
175
200
225
250
275
300
Temperature (K)
Ln = Y
Ln = Yb

Figure 4.5.

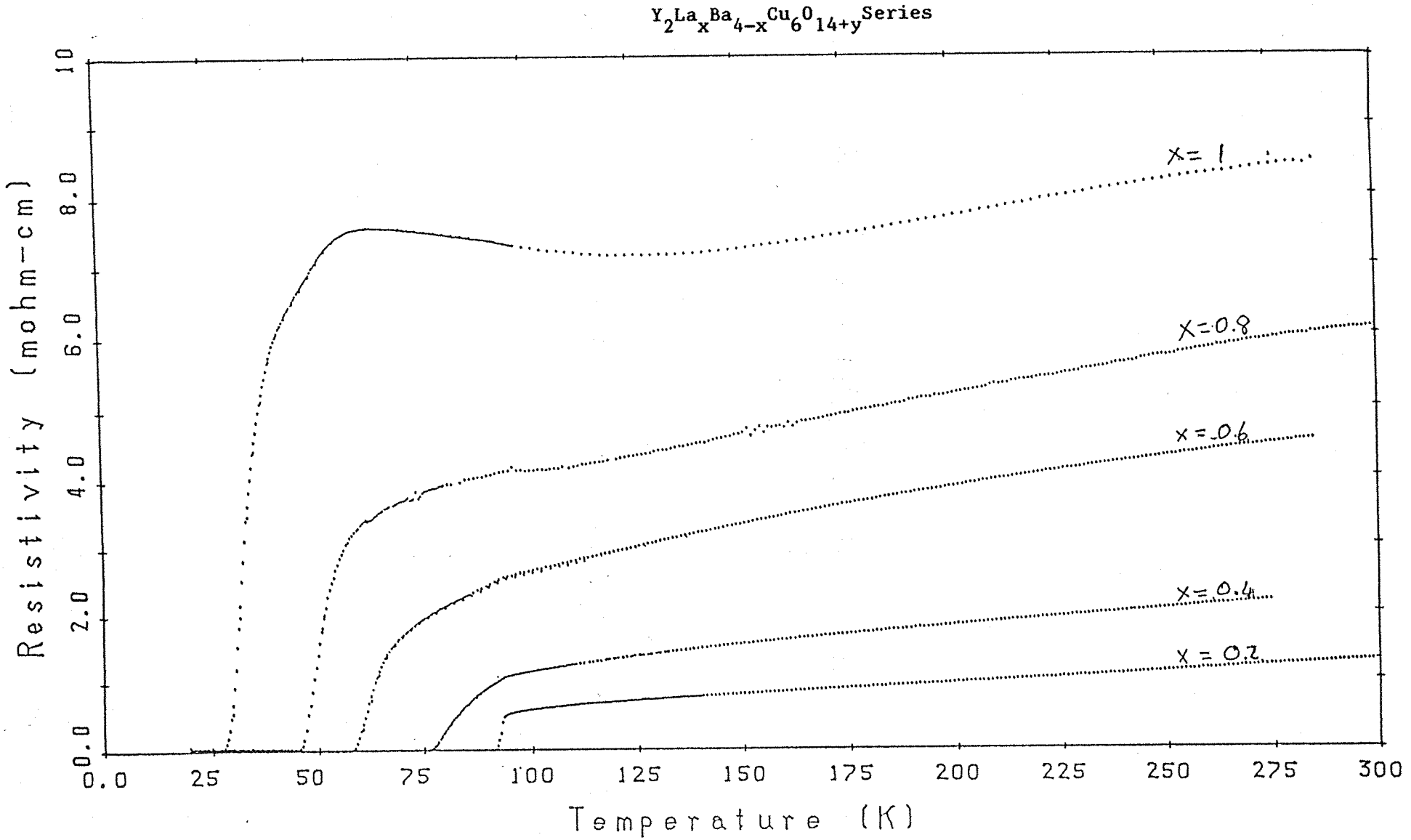
$Y_2La_xBa_{4-x}Cu_6O_{14+y}$ Series
Resistivity (mohm-cm)
Temperature (K)
0.0
2.0
4.0
6.0
8.0
10
0.0
25
50
75
100
125
150
175
200
225
250
275
300
x= 1
x=0.8
x=0.6
x=0.4
x=0.2

Figure 4.6.

In all these measurements no hysteresis in resistivity was observed.

Table II. Transition temperature T_c of $Y_nLa_{2-n+x}Ba_{4-x}Cu_6O_{14\pm y}$ (n=2,0) compounds.

Composition	T_c(K)
$Y_2La_{0.2}Ba_{3.8}Cu_6O_{13.92}$	93
$Y_2La_{0.6}Ba_{3.4}Cu_6O_{14.07}$	60
$La_2Ba_4Cu_6O_{13.8}$	65
$La_{2.2}Ba_{3.8}Cu_6O_{13.86}$	52
$La_{2.4}Ba_{3.6}Cu_6O_{14.01}$	39
$La_{2.6}Ba_{3.4}Cu_6O_{14.06}$	26
$La_{2.8}Ba_{3.2}Cu_6O_{14.07}$	(13) not superconducting down to 6K.

b. Interpretation of Resistivity Data

The structural data obtained by neutron diffraction studies and the oxygen stoichiometries obtained by thermogravimetric analysis (M T Weller, & J Grasmeder, 1987), have been studied to relate the superconducting behaviour to the structural aspects and to understand the mechanism responsible for superconductivity.

The superconducting compounds listed in Table II form a solid solution and have the formula $Y_nLa_{2-n+x}Ba_{4-x}Cu_6O_{14+y}$ (n=0,2). $Y_2Ba_4Cu_6O_{13.9}$ has an orthorhombic structure and has its T_c at 93K (P.C. Lanchester, 1987). When a small percentage of La is introduced, keeping the yttrium constant, T_c is not very much altered. T_c of $Y_2La_{0.2}Ba_{3.8}Cu_6O_{13.92}$ is 93K. As the La concentration gradually increases from x=0.2 to x=1.0 T_c falls from 93K to 23K (P.C. Lanchester, 1987).

For an eight-fold coordination of oxygen atoms, the ionic radii of Y, La and Ba are 1.155Å, 1.32Å and 1.56Å respectively. On complete replacement of Y by La in the tripled perovskite structure of $Y_2Ba_4Cu_6O_{14}$, the lattice parameter c changes from 11.67Å to 11.78Å. When La ions occupy the central A sites, they do not affect the one-dimensional chains drastically. The superconductivity in this compound $La_2Ba_4Cu_6O_{13.8}$ occurs at $\approx$ 65K and this transition temperature is very much higher than the transition temperature of $La_{2-x}Ba_xCuO_{4-y}$ (K_2NiF_4 type). The high T_c phase has a high concentration of Cu compared to the $La_{2-x}Ba_xCuO_{4-y}$ phase. The oxygen stoichiometry factors in the two high T_c compounds $Y_2Ba_4Cu_6O_{14+y}$ and $La_2Ba_4Cu_6O_{14\pm y}$ are of the same order.

The La and Ba ions are incorporated in the tripled perovskite structure as La^{3+} and Ba^{2+}. The oxygen vacancies O(5) in $Y_2Ba_4Cu_6O_{14}$ run parallel to the Cu-O chains. As La ions are gradually introduced into the two systems $La_2Ba_4Cu_6O_{14}$ and $Y_2Ba_4Cu_6O_{14}$ (Figures 4.2 to 4.4 and 4.6) the ratio La^{3+}:Ba^{2+} changes. The oxidation state of La is enhanced. Since the charge neutrality

has to be maintained, the Cu oxidation state decreases. Thus the ratio Cu^{3+}:Cu^{2+} decreases and results in a decrease of T_c. It has been clear from the characteristics of $YBa_2Cu_3O_{7-y}$ that the one-dimensional Cu-O chains play a dominant role in superconductivity. The excess La ions occupy the Ba sites. As the Ba sites are very close to the Cu-O chains, the occupancy of Ba sites by La have a deteriorating effect. Thus the reduction in T_c is expected. The formal charge valence of Cu is ≥ 2.25 in all the superconducting compounds listed in Table II. The oxygen stoichiometry factor y is below ≈ 0.2. When the oxygen concentration increases, they occupy the sites between Cu_1 ions in the basal plane and disrupt the square planar Cu-O chains.

The semiconducting behaviour of the unannealed compounds is due to the low oxidation state of Cu. The Cu oxidation state in these compounds is < 2.25.

Another important characteristic feature is obtained from the neutron diffraction results. The structures of $Y_2La_xBa_{4-x}Cu_6O_{14\pm y}$ and $La_{2+x}Ba_{4-x}Cu_6O_{14\pm y}$ exhibiting the highest T_c are orthorhombic. As the La concentration increases, the orthorhombicity decreases. The ordering of the oxygen ions significantly affects the lattice parameters. Some tetragonal structures are also found to be superconducting in spite of the link between the Cu-O chains. This observation suggests that some oxygen vacancies O(5) still exist and allow for conduction.

The compound with x=0.8 is not superconducting and at this stage the compound is approaching the orthorhombic to tetragonal transition. It tends to go to the zero resistivity state at zero K. This behaviour suggests a gradual filling up of oxygen vacancies O(5) and the disruption of the square planar chains.

In spite of a higher Cu oxidation state (> 2.25) $La_3Ba_3Cu_6O_{14.37}$ exhibits a pure semiconducting behaviour. As all the O(5) sites in this structure are filled, CuO_6 octahedra are

formed. The oxygen stoichiometry factor being much greater than 14 in this compound, the oxygen ions get localized. The charge carriers are trapped in the Cud $_{x^2 - y^2}$ band.

In the $La_{1.5}(Ln)_{1.5}Ba_3Cu_6O_{14}$ compounds Y^{3+} can fully replace the La^{3+} ion. Yb^{3+} can fully substitute for La^{3+} ion. The formal valence of copper is less than 2.25 in these compounds (Fig.4.5).

F Herman et al (1987) show that as the oxygen concentration in $YBa_2Cu_3O_{7-y}$ increases there is variation in the electronic band structure. The asymmetry in the band structure of $YBa_2Cu_3O_{7-y}$ due to the occupation of O(4) and O(5) sites is greater than the asymmetry due to the change in the lattice parameters a and b by 2%. As the Y,Ba and Cu (4s) orbitals lie much above the Fermi energy E_F, they do not play an important role in superconductivity. The orbitals below the Fermi level are Cu $3d^5$ and O $2s^2,2p^6$. The electronic density of states $N(E_F)$ is 6.6 state /eV cell.

The interaction between the Y and Ba atomic orbitals with the occupied Cu and O orbitals is very small. The O(2), O(3) and O(1) ions have almost the same number of valence charges in all the three compositions $YBa_2Cu_3O_y$, where y=6,7 and 8. The valence charges carried by Cu(1) and Cu(2) ions are different in all the three stoichiometric compounds. The chemical bonding between the Cu and O ions differs due to the difference in coordination numbers. Thus there is variation in the valence charges of Cu. As the stoichiometric factor y increases from 6 to 8, the electronic density of states near E_F increases. If the value of y is fixed, the electronic density of states $N(E_F)$ increases with the order of oxygen vacancies. The analysis of F Herman et al suggests that it may be possible to further enhance the transition temperature by increasing the oxygen content while having maximum order in the oxygen vacancies.

From our experimental results it is clear that the structure of $La_{2+x}Ba_{4-x}Cu_6O_{14\pm y}$ is similar to that of $YBa_2Cu_3O_{7\pm y}$. The oxygen vacancies O(5) play a very important role. Even though the stoichiometry of $La_{1.5}Y_{1.5}Ba_3Cu_6O_{14.0}$ is the same as that of $YBa_2Cu_3O_7$, the compound is semiconducting. Hence, the Cu oxidation state is equally important. When the formal valence of Cu $\approx$ 2.25 and the average oxygen stoichiometry factor is less than $\approx$ 0.2 the compounds are superconducting. Maximum order in the oxygen vacancies between the square planar chains results in high transition temperatures. In fact, it is possible to enhance the transition temperature in the La-Ba-Cu-O system to 90K by slightly varying the processing parameters. Zero resistivity at 80K has been observed in $LaBa_2Cu_3O_y$ (Maeda et al, 1987).

Since the presence of square planar Cu-O chains is very essential, the low dimensional behaviour of superconductivity is apparent from the experimental data.

c. a.c. susceptibility of $La_{2+x}Ba_{4-x}Cu_6O_{14\pm y}$ and $YBa_2Cu_3O_7$

The a.c. susceptibility of the samples were measured using the set up described in chapter 3. Since the unannealed samples showed a complex resistivity behaviour, compared to the annealed samples, one from each set was chosen for a.c. susceptibility measurement. The a.c. susceptibility of the following compounds have been measured.

1. $La_2Ba_4Cu_6O_{14\pm y}$
2. $La_{2.2}Ba_{3.8}Cu_6O_{14\pm y}$
3. $YBa_2Cu_3O_7$.

The magnetic response of the above compounds in an a.c. field of $\approx$ 0.15 Oe was measured and the transition characteristics are as shown in figures 4.7 and 4.8. The output across the secondary of

the mutual inductance system was compared with the signal generated by a lead sample of similar dimensions. The random errors in the calibration was found to be ± 5%. In the superconducting samples, the magnetic flux exclusion results from both the Meissner effect and the shielding effect. Hence, the observed diamagnetic shift corresponds to the upper limit of the superconducting volume fraction of the sample. The diamagnetic susceptibility of the sample increases as the temperature decreases.

The signals generated by the superconducting $La_2Ba_4Cu_6O_{14+y}$ (fig 4.7) are much smaller compared to the signals obtained by $YBa_2Cu_3O_7$ (fig 4.8). The apparent density of the material ($5.8g/cm^3$) was obtained by the measured mass and volume. The magnetic flux exclusion at 25K corresponds to about 50% of the volume of the sample. The temperature corresponding to the onset of diamagnetic response is 57K. In $La_{2.2}Ba_{3.8}Cu_6O_{14+y}$, the onset of diamagnetic response occurs at 51K.

The a.c. susceptibility of $YBa_2Cu_3O_7$ was measured using another system of mutual inductance coils. The system has not yet been calibrated. $YBa_2Cu_3O_7$ yields a large diamagnetic signal below its transition temperature. The density of the sample is taken as $6.3g/cm^3$ (from X-ray data). The magnitude of the signal obtained using the previous set of mutual inductance coils indicates that almost the whole sample is in the superconducting state. The temperature at which the onset of diamagnetism is seen agrees with the temperature corresponding to the onset of superconductivity.

The susceptibility data were taken while cooling and warming the sample and there is no indication of any hysteresis. There were no frequency dependences of χ' between 50 Hz and 300 Hz. Systematic errors involved remain almost constant over the whole temperature range. At very low temperatures, the quadrature component of the signal increases and the in phase signal decreases probably due to

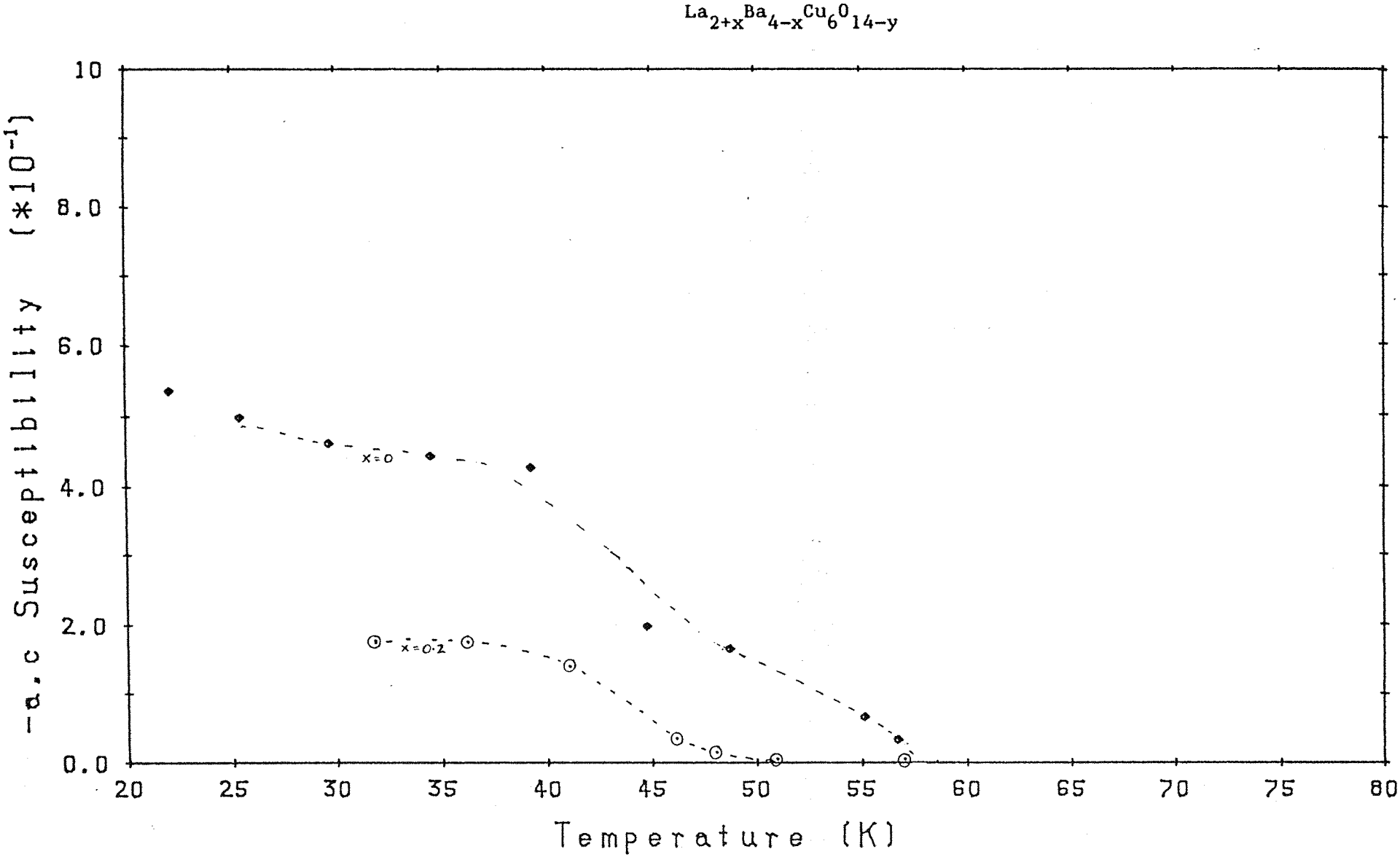
$La_{2+x}Ba_{4-x}Cu_6O_{14-y}$
-a.c Susceptibility (*10⁻¹)
10
8.0
6.0
4.0
2.0
0.0
20
25
30
35
40
45
50
55
60
65
70
75
80
Temperature (K)
x=0
x=0.2

Figure 4.7.

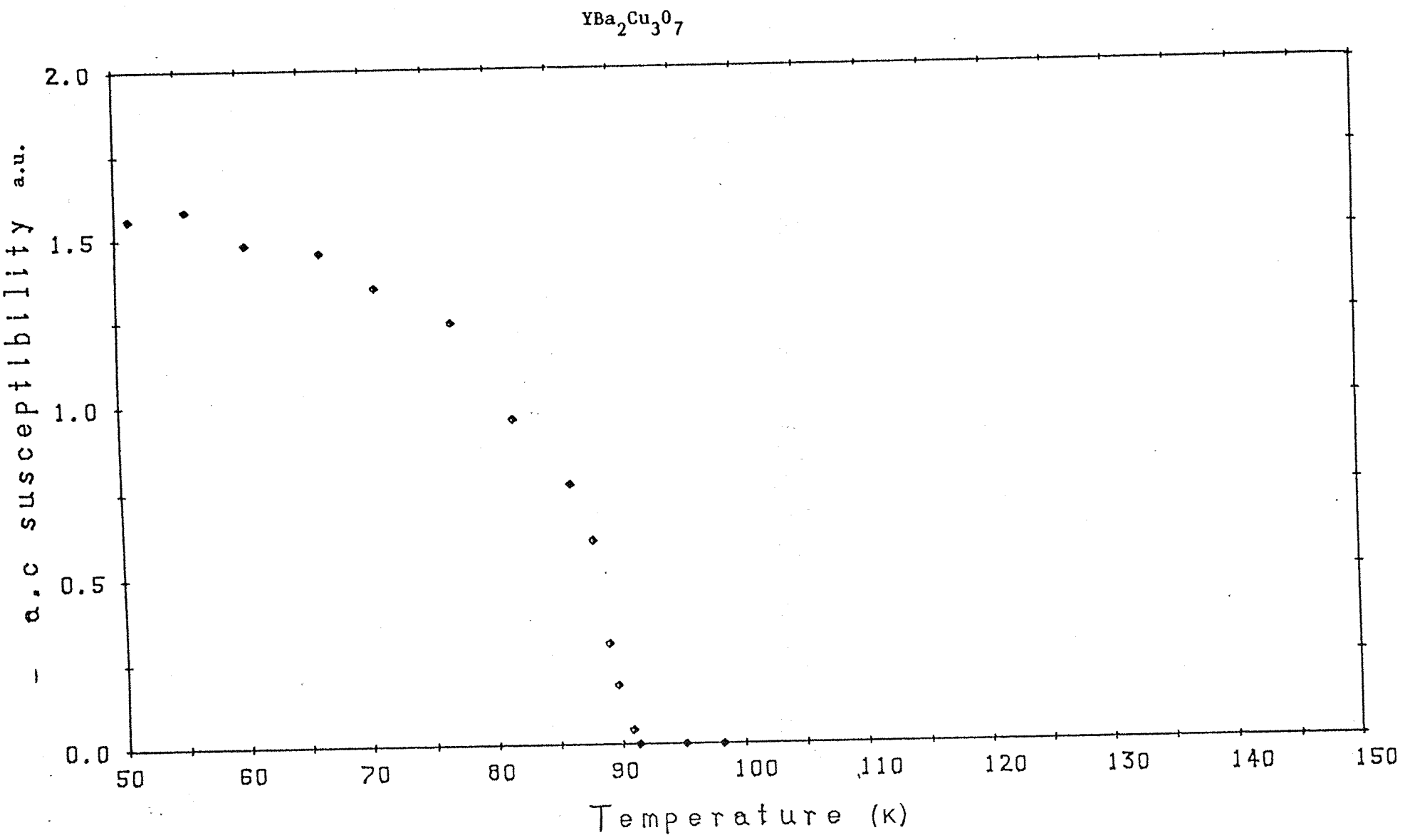
$YBa_2Cu_3O_7$
2.0
1.5
1.0
0.5
0.0
- a.c susceptibility a.u.
50
60
70
80
90
100
110
120
130
140
150
Temperature (K)

Figure 4.8.

the phase shifts in the coils or in the drive system. A dip in χ' was observed only at very low temperatures although the resultant of the two signals was a constant.

d. Thermal expansion of $YBa_2Cu_3O_7$

The thermal expansion of $YBa_2Cu_3O_7$ has been measured in the temperature range 80K to 235K. From this, the pressure dependence of the critical temperature has been estimated.

A single phase compound $YBa_2Cu_3O_7$ was prepared by taking high purity (99.99%) oxides $BaCO_3$, Y_2O_3 and CuO. These oxides (as supplied by Johnson Matthey Chemicals) were dried at 110^oC. The correct stoichiometric amounts of these oxides were ground thoroughly and heated at 950^oC in air for 24 hours in a furnace. During this heating procedure, the mixture was taken out of the furnace for periodic grindings and returned to the furnace. This mixture was then pressed into a pellet and was heated at 900^oC in a tube furnace for 48 hours in pure oxygen. The compound was finally cooled to room temperature at a rate of 3^oc/minute.

A knowledge of thermal properties like thermal expansion and specific heat is useful in investigating the mechanism responsible for the superconducting phase transition. The measurement of thermal expansion provides information regarding the thermodynamic state and the dimensional changes of the specimen. We can relate the thermodynamic variables pressure, volume and temperature (P,V,T) in the following way:

$$\beta = \left(\frac{\partial \ln V}{\partial T} \right)_p$$

where β is the volume expansion coefficient of the material. For cubic and isotropic solids $\beta = 3\alpha$.

The heat capacity C and the volume coefficient of expansion β are linked by the dimensionless Grüneissen parameter

$$\Gamma = - \left(\frac{\partial \ln T}{\partial \ln V} \right)_S = \frac{3\alpha BV}{C}$$

where α is the coefficient of linear expansion, B is the bulk modulus and S is the entropy of the lattice.

Each individual mode of vibration of frequency ω depends on the volume V and the microscopic value

$$\Gamma_i = - \frac{d \ln \omega_i}{d \ln V}$$

The anisotropic behaviour of thermal expansion is given by determining the Grüneissen parameter. In the case of superconductors, the free energy and the entropy of the system are affected by the cooperative phenomena associated with the pairing of the electrons. The superconducting transition is associated with an anomaly or jump in thermal expansion.

The thickness of the pellet used for determining the expansivity was 0.3cm. The relative length changes $\Delta\ell/\ell$ of the sample for 80K< T < 100 K are as shown in figure 4.9. The variation of expansivity of the sample with temperature is as shown in figure 4.10.

The details of the experimental procedure are given in chapter 3. The sample was allowed to cool gradually to 70K and the flow of helium into the exchanger space was controlled, so that the sample started warming up gradually. The rate of increase in temperature of the sample could be maintained constant by careful adjustment of the flow valve for about two hours. The heating rate was adjusted to about 1mK/sec. The temperature of the sample increased by another 9 or 10K during this period of adjustment. We were interested in the thermal expansion behaviour near T_c. Thus the temperature of interest was chosen at 90K.

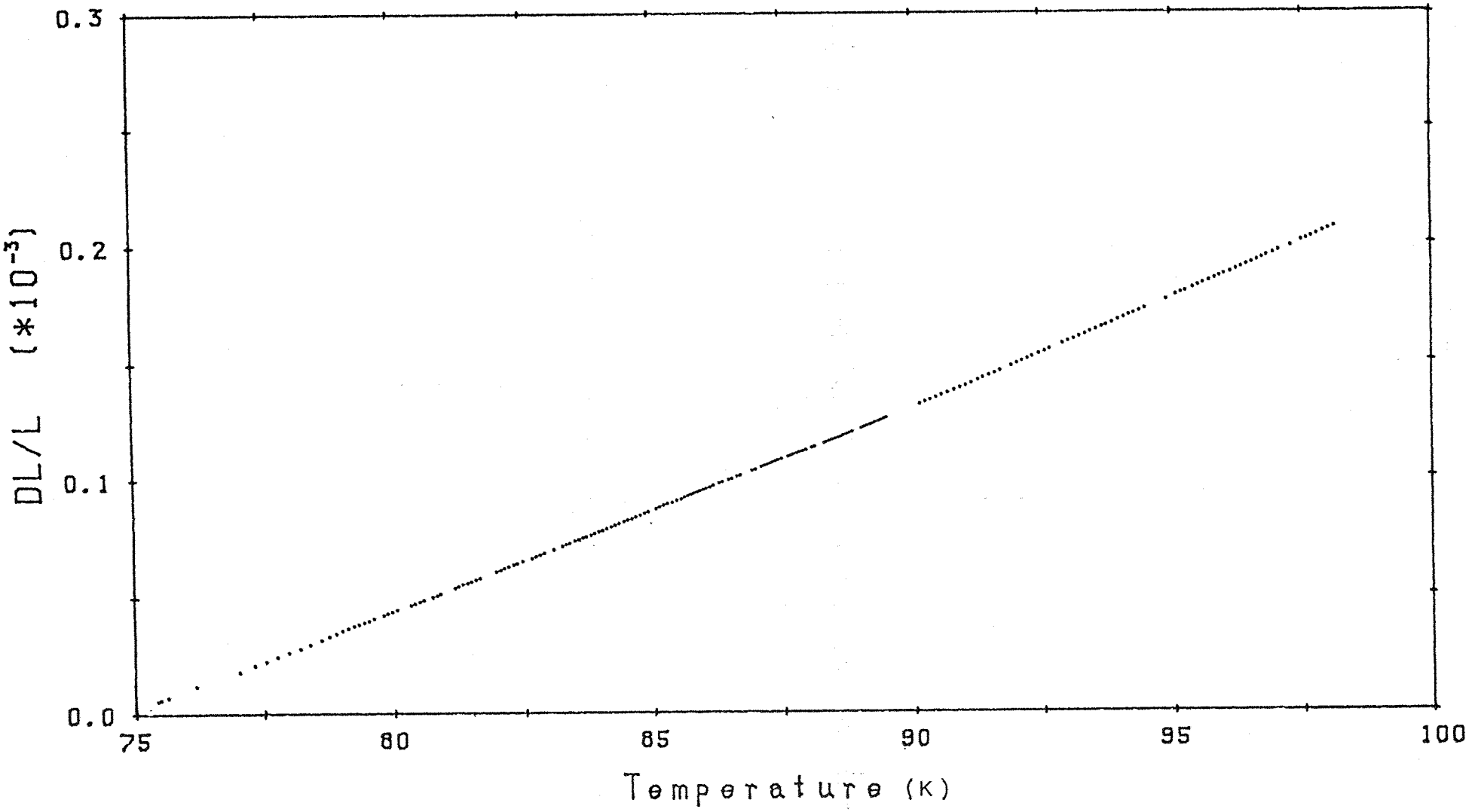

Figure 4.9.

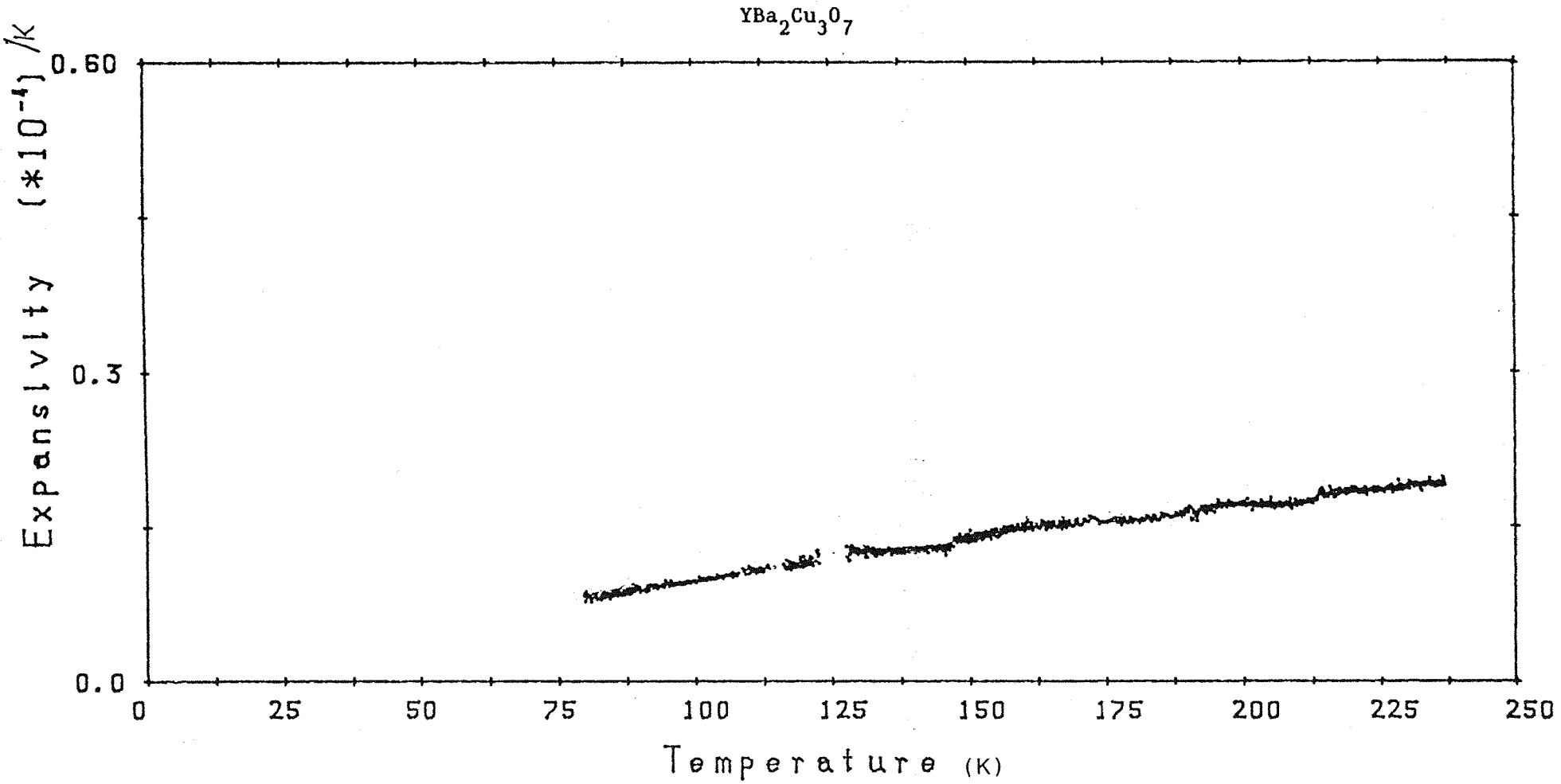
YBa2Cu3O7
Expanslvlty (*10-4) /K
0.60
0.3
0.0
0
25
50
75
100
125
150
175
200
225
250
Temperature (K)

Figure 4.10.

The thermal expansion data do not show any remarkable change at T_c (Fig.4.10). The temperature resolution was 0.1K in this measurement. The rate of variation of α with temperature is very small. There is considerable scattering in the data throughout the temperature range whereas less scattering was observed in the data obtained for intermetallic polycrystalline compounds. The absence of data points around 125K is due to a disturbance in the electrical mains. The value of α in the normal state is greater than that in the superconducting state. At $T_c \approx 91K$, the thermal expansivity is given by

$$\alpha = (9.36 \pm 0.08) \times 10^{-6}/K.$$

On comparing this value with our measurements on the expansion of GdCu, we find that the expansivity of $YBa_2Cu_3O_7$ is an order of magnitude less than that of GdCu. We made use of the same expansion cell for both the measurements. Compounds like GdCu have the CsCl structure. An anomaly obtained in the resistivity data of GdCu is due to a transition from a paramagnetic to an antiferromagnetic state (Chao,1966). At $T_c \approx 137K$,

$$\alpha \approx (1.32 \pm 0.02) \times 10^{-5}/K$$

and an anomaly is seen in the thermal expansion data. The resolution in the measurements of α of $YBa_2Cu_3O_7$ is $3 \times 10^{-8}/K$. In the case of GdCu, the resolution obtained was $1 \times 10^{-7}/K$.

The thermal expansion of $YBa_2Cu_3O_7$ determined by the measurement of X-ray diffraction lines in the temperature range -173K to 300K is found to be very small and anisotropic (Almond et al 1987). In ceramic materials the anisotropic behaviour of thermal expansion is the potential cause for microfracture occurring at grain boundaries. In the case of hot pressed materials, the applied stress during fabrication might affect the structural homogeneity of the material. The amount of cracking increases as the temperature of the sample decreases. The uncertainty in the measurement of α may be

due to the effect of size of the grains and the porosity of the sintered sample on its mechanical behaviour. The density may not be the same throughout the volume of the sample and the dilatometer may be yielding the data only on a part of the sample. In brittle heterogeneous ceramic materials, an increase in microfracture results in decreasing the thermal expansion coefficient. The thermal expansion measured of this sample may be attributed to the average behaviour over those occuring in different directions.

Although an anomalous behaviour of thermal expansion at T_c has not been observed, we try to consider the change in the value of α at T_c in the normal and superconducting states and determine the variation of critical temperature with pressure (Bayot et al, 1987). Form our data, we can give an upper limit to the difference in α as

$$\alpha_n - \alpha_s \leqslant 0.1 \times 10^{-6}/K.$$

Hence, $$\beta_n - \beta_s \lesssim 3 \times 10^{-7}/K$$

The change in the value of the volume coefficient and the variation of the thermodynamical critical field with pressure and temperature at the critical point are related (Lynton E A, 1967).

$$\beta_n - \beta_s = \frac{1}{\mu_o} \left(\frac{\partial B_c}{\partial p} \right)_{T_c} \left(\frac{\partial B_c}{\partial T} \right)_{T_c} \qquad (1)$$

where β_n and β_s are the volume expansion coefficients in the normal and superconducting states.

At $T = T_c$, $B_c = 0$

$$\left(\frac{\partial B_c}{\partial p} \right)_{T_c} = - \left(\frac{\partial B_c}{\partial T} \right)_{T_c} \left(\frac{\partial T_c}{\partial p} \right)_{B_c} = 0$$

substituting for $\left(\frac{\partial B_c}{\partial p} \right)_{T_c}$ in (1),

$$\beta_n - \beta_s = -\frac{1}{\mu_o} \left(\frac{\partial B_c}{\partial T} \right)^2 \left(\frac{\partial T_c}{\partial p} \right) \qquad (2)$$

From the magnetization measurements of Cava et al (1987b), $B_c(0) = 1T$.

$\frac{\partial B_c}{\partial T}$ is estimated by assuming a parabolic temperature dependence for $B_c(T)$.

$$B_c(T) = B_c(0) \left\{ 1 - \left(\frac{T}{T_c} \right)^2 \right\}$$

Substituting for $\beta_n - \beta_s$, $\partial B_c / \partial T$ and μ_o in (2),

$$\frac{dT_c}{dp} \lesssim 0.078 \text{ K/kbar}$$

The result implies that the pressure dependence of critical temperature is very small.

A.Driessen et al (1987a) have studied the pressure dependence of T_c in $YBa_2Cu_3O_{9-y}$ ($y \approx 2$) by subjecting the sample upto a pressure of 170 kbar. As the pressure increases, T_{co} increases and T_{cf} (corresponding to zero resistivity state) decreases. They obtain a value for dT_c/dP as equal to 0.043K/kbar. Bayot et al obtain an upper limit of dTc/dP as 0.13K/kbar.

5. CONCLUSION

The discovery of superconductivity in La-Ba-Cu-O systems by Bednorz and Müller made a break through in the field of superconductivity. In spite of the tremendous development that has been made both on the experimental and theoretical side, thorough investigations of the properties of these materials are very essential to understand the mechanism underlying their superconducting behaviour.

From our thermal expansion measurements on $YBa_2Cu_3O_7$, we find that the expansivity is very small and increases with temperature. To observe any detectable anomaly at T_c, it is very essential to conduct measurements on single crystals of these materials. The expansivity of our measurement is of the same order as determined by Driessen et al (1987b). Driessen et al have estimated the Grüneissen parameter Γ. Γ depends slightly on temperature below T_c and is temperature independent above T_c. This shows that the volume dependence of the individual lattice vibrations does not vary much.

From our results (chapter 4) deduced using thermodynamics, we find that pressure has only a slight effect on changing the transition temperature. Driessen et al have studied the variation of T_c with pressure using the BCS model. This model accounts for the high transition temperatures in compounds having large values of the electron-phonon interaction parameter λ (Allen and Dynes, 1975). $\partial \ln T_c/\partial p$ along with other parameters Γ and B provides information on λ. The variation of T_c with λ is given by

$$k_B T_c = \frac{\hbar\omega_{log}}{1.2} f_1 f_2 \exp\left\{ \frac{-1.04(1+\lambda)}{\lambda-\mu^*(1+0.62)\lambda} \right\}$$

where ω_{log} is the weighted average of the electron-phonon spectral function. μ^* is the effective coulomb interaction. f_1 and f_2 are parameters depending on the value of λ. Driessen et al express T_c as a function of λ only. Substituting for T_c, they arrive at $\lambda = 4.7$. The variation of T_c with pressure p has been given as:

$$\frac{\partial \ln T_c}{\partial p} = \frac{1}{B}\left[\Gamma_{log} - g(\lambda)\frac{\partial \ln \lambda}{\partial \ln V}\right]$$

For $1.5 \leqslant \lambda \leqslant 10$, $g(\lambda)$ has been given by $g(\lambda) \simeq 0.4 + \frac{1}{\lambda}$.

Substituting the experimental values of the bulk modulus B and the Grüneissen constant Γ_{log}

$$\frac{\partial \ln \lambda}{\partial \ln V} = 2.8$$

The above relation obtained by assuming the BCS model implies that the electron-phonon interaction decreases with pressure (Driessen et al, 1987).

Our resistivity measurements on the unannealed and annealed $La_{2+x}Ba_{4-x}Cu_6O_{14\pm y}$ compounds show that T_c is very sensitive to the oxygen stoichiometry. The processing parameters being kept the same, an increase in the La concentration of $Y_2La_xBa_{4-x}Cu_6O_{14\pm y}$ results in reducing the copper oxidation state and change the oxygen stoichiometry factor. The reduction in T_c has been explained as due to the disruption of the square-planar chains which are one-dimensional in character. If the square-planar chains are entirely responsible for the conducting path, the one-dimensional behaviour should also be evident in the measurement of the coherence length ξ. The coherence lengths measured along the direction of the chains should be greater than those measured in the directions normal to the chains. The coherence lengths have been derived from the magnetization data on single crystals of $YBa_2Cu_3O_{7-y}$ by W.Gallagher et al (1987). The twinning effect in the a-b plane causes the distribution in these directions. Thus an anisotropic behaviour that may exist in the a-b plane will not be apparent. When the CuO planes are mounted perpendicular and parallel to the applied field, the values of ξ have been found to be 4.3Å and 31Å respectively. i.e., the coherence length normal to the CuO planes is 4.3Å. This has been compared with the distance between the Cu-O layers (adjacent to the Y layer) and the distance between the square planar Cu-O chains. From the characteristics of the coherence length, the

authors show that the macroscopic properties are three dimensional in character.

The resistivities of the series of superconducting compounds $La_{2+x}Ba_{4-x}Cu_6O_{14\pm y}$ ($0.2 < x < 0.8$) and $Y_2La_xBa_{4-x}Cu_6O_{14\pm y}$ ($0.2 < x < 1.0$)at room temperature are less than 10 mΩ cm. The stoichiometry of $Y_2Ba_4Cu_6O_{14\pm y}$ is the same as that of $Y_{0.33}Ba_{0.67}CuO_{2.33\pm y}$. Rao et al (1987) find that the resistivity of the superconducting $Y_{0.33}Ba_{0.67}CuO_{2.33\pm y}$ at room temperature is close to a metal-nonmetal transition.

The Cu(1) ions associated with the square planar chains seem to play an important role in all the superconducting oxides studied so far. To elucidate the properties associated with the Cu-O chains Cu ions have been partially substituted by 3d ions like Cr, Mn, Fe, Co, Ni and Zn. A decrease in T_c has been observed in all these compounds (S B Oseroff et al, 1987). Although Zn^{2+} is nonmagnetic, it depresses the transition temperature to a larger extent than the other ions. The decrease in T_c cannot be related to the magnetic moment of the 3d ion. The crystal field at the Cu(1) and Cu(2) sites can be estimated by considering the electrostatic interactions, charge transfer excitations and the isotropic property of the interactions between the d-orbitals (L.E. Orgel, 1966). The difference in the crystal field stabilization energy has been shown to have a strong correlation with T_c (M W C Dharmavardana, 1987). T_c is lowered when a 3d ion occupies the Cu(1) site.

Our a.c. susceptibility measurements on the unannealed $La_{2.2}Ba_{3.8}Cu_6O_{14}$ show that the superconducting property exists in a minority phase of the sample. No clue for the existence of this phase is obtained from the complex resistivity behaviour of the unannealed samples. Thus the a.c. susceptibility measurements became one of our major methods of fast characterization of the new superconducting materials.

The field of high temperature superconductivity in oxide ceramics is still in its initial stage. The enormous efforts from the theoretical and experimental research groups are being directed towards achieving higher T_c superconductors. It is interesting to note that a mixed phase of Y-Ba-Cu-O has resistive transitions at 240K and 90K from the data of Chen et al (1987). This anomaly has been suggested as due to a second phase (rich in Cu) in addition to the orthorhombic phase (Narayan et al, 1987). The new phase is destroyed on subjecting the specimen to low temperature cycling. This anomalous behaviour could also be due to the antiferromagnetic ordering of CuO (B Roden et al, 1987). The results reported at 240K have not been found reproducible. Superconductivity at $65^{o}C$ was reported in $Sr_xBa_{2-x}YCu_3O_{7-y}$ for x = 1.0 by Ihara et al (1987). Recently there have been reports from Chu et al (1988) regarding the discovery of superconductivity in $BiCaSrCuO_x$ with $T_c \approx 120K$. The increasing interest in the investigation of these compounds show that the days for using room temperature superconductors may not be far off.

The magnetization measurements suggest that it is possible to fabricate good quality superconductors capable of carrying high electric currents in high magnetic fields. The critical field at zero K might exceed 50T in these materials. This value is much larger compared to the critical field of Nb_3Sn.

The high T_c superconductors are expected to have numerous applications in high power and electronic technology. Electrical power transmission will be possible without resistive losses. Electric machinery based on liquid nitrogen cooled superconductors are more beneficial compared to the high cost involved in maintaining the vacuum systems that are being used for the helium cooled superconductors.

REFERENCES

Almond D P, Bullett D W, Chapman B, Cooke R G, Dawson W G, Draper R C J, Ford P J, Hampton R N, Wang Hong, Lambson E F, Saunders G A and Sullivan R A L (1987) Proc. of Genoa Conf. on High Temperature Superconductivity, 379-380.

Allen P B and Dynes R C (1975) Phys.Rev. B12 905.

Anderson D (1987) Science 235 1196-1198.

Balakrishnan G, Bernhoeft N R, Bowden Z A, McK-Paul D and Taylor A D (1987) Nature 327 45-47.

Barren T H K, Collins J G and White G K (1980) Adv.in Phys. 29(4) 609.

Batlogg B, Kourouklis G, Weber W, Cava R J, Jayaraman A, White A E, Short K T, Rupp L W and Rietman E A (1987) Phys.Rev.Lett. 59 912-914.

Bardeen J, Schriefer J R and Cooper L N (1957) Phys.Rev. 106 162; 108 1175.

Bayot V, Dewitte C, Erauns J P, Gonze X, Lambricht M and Michenaud JP (1987) Solid State Commu. 64 327.

Bednorz G J and Müller K A (1986) Z.Phys. B64 189-193.

Bednorz G J and Müller K A (1987a) Solid State Comm. 64 380-384.

Beech F, Miraglia S, Santoro A and Roth R S (1987) Phys.Rev.B, 8778-8780

Bordet P, Chaillout C, Capponi J J, Chenavas J and Marezio M (1987) Nature 327 687-689.

Cava R J, Van Dover R B, Batlogg B and Rietman E A (1987a) Phys.Rev.Lett. 58 408.

Cava R J, Batlogg B, Van Dover R B, Murphy D W, Sunshine S, Siegrist T, Remeika J P, Rietman E A, Zahurak S and Espinosa G P (1987b) Phys.Rev.Lett. 58 1676-1679.

Cava R J (1987c) Proc. of Genoa Conf. on High Temperature Superconductivity 233-240.

Chao C C (1966) J. of Appl.Phys. 37 2081-2084.

Chen J T, Wenger L E, McEvan C J and Logothetis E M (1987) Phys.Rev.Lett. 58 1972.

Chu C W, Hor P H, Meng R L, Gao L, Huang Z J and Wang Y Q (1987) Phys.Rev.Lett. 58 405-407.

Corak W S and Satterthwaite C B (1954) Phys.Rev. 99 1660.

David W I F, Harrison W T A, Ibberson R M, Weller M T, Grasmeder J R and Lanchester P C (1987) Nature 328, 328-329.

de Groot P A J, Rainford B D, McK-Paul D, Lanchester P C, Weller M T and Balakrishnan G (1987) J.of Phys.F (GB) 17 PL 185-8.

Dharmavardana M W C (1987) Phys.Lett.A 126 205-207.

Driessen A, Griessen R, Koeman N, Salomons E, Brouwer R, de Groot D Heeck K, Hemmes H and Rector J (1987a) Phys.Rev.B 36 5602.

Er-Rakho L, Michel C, Provost J and Ravean B (1981) J.Solid State Chem. 37 151-156.

Freeman A J, Jaejun Yu and Xu J H (1987) Phys.Rev.Letts. 58 1035-1037.

Freeman A J, Yu JJ, Massida S and Koelling D (1987) Phs.Lett.A 122 198.

Galasso F S (1970) Structures of inorganic solids.

Gallagher W J, Worthington T K, Dinger T R, Holtzberg F, Kaiser D L and Sandstrom R L (1987) Physica 148B 228-232.

Gaveler J R (1973) Appl.Phys.Lett. (USA) 23 480-482.

Ginzburg V L and Landau L D (1950) Zh.Eksp.Teor.Fiz. 20 1064.

Gorter C J and Casimir H B G (1934) Phys.Z 35 963; Z.Tech.Phys. 15 539.

Grant P M, Parkin S S P, Lee V Y, Engler E M, Ramirez M L, Vazquez J E, Lim G and Jacowitz R D and Greene R L (1987) Phys.Rev.Lett. 58 2482-2485.

Herman F, Kasowski R V and Hsu W Y (1987) Phys.Rev.B 36 6904-6913.

Hock K H, Nickisch H, Thomas H (1983) Helv.Phys. Acta 56 237.

Hor P H, Ga OL, Meng RL, Huang Z J, Wang YQ, Forster K, Vassilious J, Chu C W, Wu M K, Ashburn J R and Torng C J Phys.Rev.Lett. 58 911 (1987a)

Hor P H, Meng R L, Chu C W, Wu M K, Zirngiebl E, Thompson J D and Huang C Y (1987b) Nature 326 669-670.

Huebener R P (Springer Series in Solid State Sciences (6) Magnetic flux structures (1978) 38.

Igra R M, Rao M G and Scurlock R G (1983) Proc. of ICEC II, Berlin, 1986 p.617-621.

Ihara H, Terada N, Jo M, Hirabayashi M, Tokumoto M, Kimura Y, Matsubara T and Sugise R (1987) J.J.A.P. 26 L1413-L1415.

Johnston D C, Prakash H, Zachariasen W H and Viswanathan R (1973) Mater.Res.Bull. 8 777.

Kamerlingh Onnes H, (1911) Akad van Wetenschappen (Amsterdam) 14 113, 818.

Kishio K, Kitazanea K, Sugii N, Kanbe S, Fueki K, Takagi H and Tanaka S (1987b) Chem.Letts. 3 547-549

Kishio K, Kitazawa K, Kanbe S, Yasuda I, Sugii N, Takagi H, Uchida S, Fueki K and Tanaka S (1987a) Chem.Lett. 2 429-432.

Kittel C (1976) Introduction to Solid State Physics, 390.

Kroeger F R and Swenson C A, (1977) J.Appl.Phys. 48(3) 853.

Lanchester P C (1987) (Private Communication).

Leary K J, Zurloye H C, Keller S W, Fattens T A, Ham W K, Michaels J N and Stacy A M (1987) Phys.Rev.Lett. 59 1236-1239.

Legg G J (1980) PhD Thesis, Southampton University.

Lynton E A (1961) Superconductivity, John Wiley & Sons, New York.

Maeda A, Yabe T, Wchinokura K and Tanaka S (1987) J.J.A.P. 26 L1368.

Matheiss L F and Hamann D R (1987) Solid State Commun. 63 395.

Maxwell E (1950) Phys.Rev. 78 477.

McK-Paul D (1987) submitted

Müller K A, Bednorz J G and Takashige M (1987b) Phys.Rev.Lett.58 1143-1146.

Mitzi D B, Marshall A F, Sun J Z, Webb D J, Beasley M R, Geballe T H and Kapitulnik A (1987) (submitted to Phys.Rev.)

Nishihira Y, Tokumato M, Murata K and Unoki H (1987) J.J.A.P. 26 L1416-1418.

Narayan J, Shukla V N, Lukasiewicz S J, Biunno N, Singh R, Schreiner A F, Pennycook S J (1987) Appl.Phys.Lett.(USA) 51 p940-2.

Orgel L E (1966) (Mathuen, London) An introduction to transition-metal chemistry : ligandfield theory.

Oseroff S B, Vier D C, Snyth J F, Salling C T, Chultz S, Dalicha O Y, Lee B W, Maple M B, Fisk Z, Thompson J D, Smith J and Zirngiebl E (1987) Solid State Comm. 64 241.

Pippard A B (1950) Proc.Roy.Soc. A 203 210.

Pulham R (1987) PhD Thesis, Southampton University.

Rainford B D (1987) (Private Communication).

Ramirez A P, Scheemeyer L F and Waszczak J V (1987) Phys.Rev. B 36 7145.

Rao C N R (1984) and Ganguly P, J Solid State Chem. 53 193.

Rao C N R, Ganguly P and Rayachoudhuri A K (1987) Nature 326 856-857.

Roden B, Braun E and Freimuth A (1987) Solid State Comm. 64 1051-1052.

Roth R S, Dennis J R and Davis K L (1987) Adv.Ceramic Mat. 2 303.

Salomens E, Hemmes H, Scholtz J J, Koeman N, Brouwer R, Driessen A, de Groot D G and Griessen R (1987b) Physica 145 B 253-259.

Schauer W, Küpfer H, Flükiger R, Apfelstedt I, Meier-Hirmer R and Wühl H (1987) Proc. of Genoa Conf. on High Temperature Superconductivity 393-394.

Scheemeyer L F, Waszczak J V, Siegrist T, Rupp L W, Batlogg B, Cava R J and Murphy D W (1987) Nature 328 601-602.

Singh K K, Ganguly P and Goodenough J B (1984) J.Solid State Chem. 52 254.

Smit H H A, Dirken M W, Thiel R C and de Jongh L J (1987) Solid State Comm. 64 695.

Spille H, Kneissel H, Rauchschwalbe I J, Steglich F, Rietschel H and Ewert F (1987) Proc. of Genoa Conf. on High Temperature Superconductivity 395.

Takagi H, Uchida S, Kitazawa K and Tanaka S (1987a) J.J.A.P. 26 L123-124.

Takagi H, Uchida S, Kitazawa K, Kishio K, Fueki K and Tanaka S Proc. of Genoa Conf. on High Temperature Superconductivity 1987b 241.

Takita K, Akinaga H, Katoh H, Uchino T, Ishigaki T and Asano H (1987) J.J.A.P. 26 L1323-L1325.

Tanenbaum M and Wright W V, (1962) Proc. of Tech.Sessions on Superconductors (New York).

Thompson A M (1958) I.R.E. Trans.Instru. 7(I) 245.

Tilford (1969) PhD Thesis, Aimes University.

Tinkham M (1975) (New York, McGraw-Hill) Introduction to Superconductivity.

Welch D O (1985) IEEE Trans.Mag. MAG-21 827.

Weller M T, Grasmeder J (Private Communication)

White G K, (1961) Cryogenics 1 151-158.

Wu M K, Ashburn J R, Torng C J, Hor P H, Meng R L, Gao L, Huang Z J, Wang Y Q and Chu C W (1987) Phys.Rev.Lett. 58 908-910.

Yamanaka A, Minami F, Watanabe K, Inoue Kuon, Takekawa S and Iyi N (1987) J.J.A.P. 26 L1404-L1406.

Acknowledgements

I sincerely thank Professor B.D.Rainford for accepting me in the Magnetism Group, for having taught magnetism in rare-earths and also for continued cheerful guidance throughout.

I am grateful to Dr P.A.J. de Groot, my supervisor, who encouraged me throughout my study to complete the project, for helpful discussion and criticism. Also I thank him for his guidance in heat capacity and magnetization measurements.

My sincere thanks are also due to Dr P.C. Lanchester for his advice and guidance in resistivity measurements; to Dr R.J. Pulham for his patience and guidance in a.c. susceptibilty and thermal expansion measurements; to Dr M.T. Weller and Mr J.R. Grasmeder for providing samples of high T_c superconductors and structural analysis; to Mr Colin Miles, Mr Mark Newman and Mr Brian Heath for their technical assistance and to Mrs Margaret Wainwright for her splendid job in transforming the manuscript into this presentable form. The cooperation from all my friends in the Magnetism Group and the Institute of Cryogenics is also very much appreciated.

I thank Professor N.G.Puttaswamy and the Mössbauer group (Bangalore University & I.I.Sc) for their encouragement;
Mr Y.Ramachandra, the Chairman and Professor Vimala Kannan, the Principal (B.M.S. College for Women, Bangalore, India) for sanctioning the leave.

I thank my parents and my husband for their encouragement and assistance throughout this work.